minerals

MDPI

Review

Engineering Zeolite Acidity and Porosity for Improved Esterification: A Review of Mechanisms, Kinetics, and Sustainability Processes

Jelena Pavlović [1] and Nevenka Rajić [2,*]

[1] Institute of Soil Science, Teodora Drajzera 7, 11000 Belgrade, Serbia; soils.pavlovic@gmail.com
[2] Faculty of Ecology and Environmental Protection, University "Union—Nikola Tesla", Cara Dušana 62–64, 11158 Belgrade, Serbia
* Correspondence: nrajic@unionnikolatesla.edu.rs; Tel.: +381-11-2180-271

Abstract

Esterification, the reaction between carboxylic acids and alcohols that produces esters and water, plays a vital role in many industries, especially in biodiesel and pharmaceutical manufacturing. Traditional methods using homogeneous mineral acids pose environmental issues, prompting the search for sustainable alternatives—solid acid catalysts. Zeolites offer unique structural advantages, including shape selectivity and adjustable acidity, which improve reaction efficiency and reduce waste. This review provides a detailed examination of how zeolite topology—particularly pore structure and connectivity—influences the kinetics of long-chain fatty acid (LCFA) esterification. It investigates the optimization of acid sites via modifications to the silicon-to-aluminum ratio (Si/Al), ion exchange, and pore engineering to improve mass transfer. The study investigates key reaction mechanisms, specifically the Langmuir–Hinshelwood (LH) and Eley–Rideal (ER) models, to address issues such as mass-transfer limitations and water inhibition. The paper highlights recent advances in sustainable catalyst design, such as hierarchical zeolites and membrane-integrated reactors, for converting biomass-derived feedstocks into valuable esters. It also discusses current research challenges and suggests future directions, including the use of 3D-printed monoliths and machine learning integration, to develop next-generation, eco-friendly zeolite catalysts.

Keywords: zeolites; solid catalysts; esterification; clinoptilolite; solid acids

Academic Editor: Andreas Delimitis

Received: 23 December 2025
Revised: 2 February 2026
Accepted: 5 February 2026
Published: 6 February 2026

1. Introduction

Esterification, the reaction of a carboxylic acid with an alcohol to produce an ester and water, is a crucial process in the chemical industry. The esters formed are valuable compounds with various uses, including as solvents [1,2], fragrances [3], flavoring components [4], pharmaceuticals [5], as well as in the food and cosmetics industries [6,7]. One primary industrial application is the production of biodiesel, a renewable fuel produced through transesterification [8,9]. In this process, triglycerides (esters from vegetable oils or animal fats) react with a simple alcohol, such as methanol [10,11] or ethanol [12,13] to produce fatty acid methyl esters (FAMEs or biodiesel).

The acid-catalyzed mechanism for this reaction, often called Fischer esterification, is shown in Figure 1 [14]. The process begins when an acid catalyst protonates the carbonyl oxygen of the carboxylic acid, increasing the electrophilicity of the carbonyl carbon. A

nucleophile attack by the alcohol on this activated carbon results in a tetrahedral intermediate. Then a series of proton transfers culminates in the protonation of a hydroxyl group, producing water, a good leaving group. The water leaves, and a final deprotonation step produces the neutral ester while regenerating the acid catalyst.

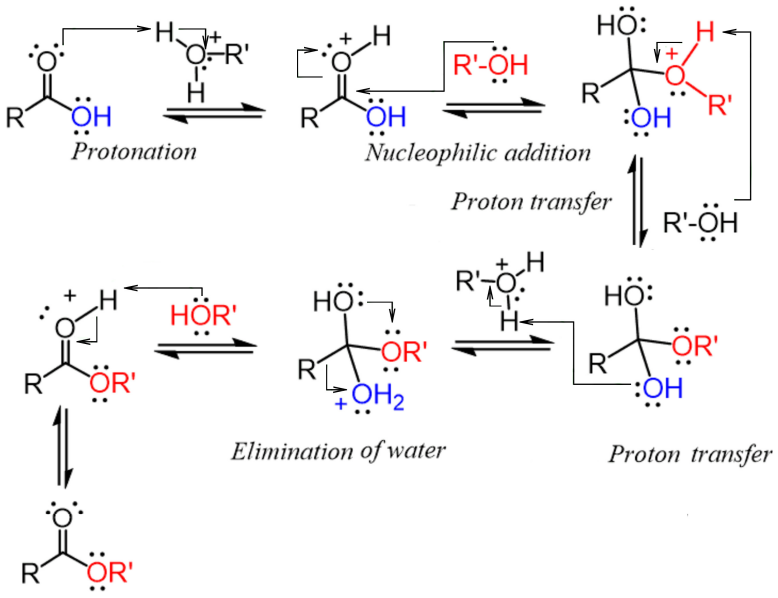

Figure 1. Schematic presentation of the Fischer esterification.

Esterification also plays a vital role in the production of polymers and plastics, where esters serve as essential monomers or additives. In the pharmaceutical industry, this process is crucial for the manufacture of many medications; for example, aspirin (acetylsalicylic acid) is produced from salicylic acid and acetic anhydride [15]. Additionally, esters such as ethyl and butyl acetate are commonly used as solvents in paints, varnishes, and adhesives, and as plasticizers to improve flexibility and reduce brittleness in plastics [16–18]. Conversely, saponification, the opposite process, is used to make soap from fats.

Traditionally, esterification is catalyzed by homogeneous mineral acids, mainly sulfuric acid (H_2SO_4). Although effective, this catalyst causes significant environmental and operational issues, including equipment corrosion, expensive neutralization, and difficulty with catalyst separation and recycling [19–21]. The development of solid acid catalysts offers a promising alternative, providing a heterogeneous, sustainable, and highly efficient method [22–26]. Solid acid catalysts function through active acidic sites on an insoluble substrate. The process involves either protonating the carbonyl oxygen of the carboxylic acid with a Brønsted acid site (such as a $–SO_3H$ group) or binding it to a Lewis acid site (such as a transition-metal ion). A key benefit of this heterogeneous approach is its simplicity. After the reaction, the catalyst can be easily removed by filtration, reducing corrosive waste streams and enabling efficient catalyst reuse. This significantly lowers both operational costs and environmental impact.

Many materials, each tailored to specific reaction conditions and reactant types, have been developed as efficient solid acid catalysts. Commonly used polymeric ion-exchange resins with highly active sulfonic acid groups ($–SO_3H$) include Nafion and Amberlyst [27–29]. Since they typically degrade above 120 °C, their low thermal stability often limits their use despite their high activity. Sulfated metal oxides, such as sulfate-modified zirconia (SO_4^{2-}/ZrO_2), are used in processes that require higher temperatures [30,31]. These materials are ideal for esterifying high-boiling-point fatty acids, a key step in biodiesel production, because their superacidity enhances reaction rates and stability under demanding thermal

conditions. However, sulfated metal oxides as super-acid catalysts face disadvantages, including leaching of active sulfate groups, deactivation due to organic deposits and water, and potential environmental concerns associated with the metals [32–34].

Zeolite-based catalysts have emerged as promising alternatives for esterification processes [35–40]. Their distinctive, homogeneous microporous architectures facilitate shape selection, while their adjustable solid-state acidity enhances stability, safety, and ease of regeneration compared to alternative solid acids. The porous architecture facilitates reactant accessibility and boosts selectivity, hence promoting process intensification and a more sustainable chemical industry. Zeolites can play a significant role as heterogeneous catalysts in esterification, offering a sustainable alternative to traditional liquid-acid methods.

The main goal of this study is to identify current research challenges and suggest future directions for developing next-generation, highly efficient, and eco-friendly zeolite catalysts for esterification. This review stands out from existing literature by examining the recent shift toward precisely engineered catalytic systems developed between 2020 and 2026, providing a unique combination of fundamental kinetics (LH and ER models) and modern technological innovations, such as 3D-printed monoliths and machine-learning-based performance predictions. The main challenge tackled in this review is the inherent conflict between zeolite acidity and the operational difficulties caused by water inhibition and internal mass-transfer limitations, which largely restrict these catalysts' industrial viability. We offer an analytical perspective on this 'diffusion bottleneck,' where bulky long-chain fatty acids (LCFAs) encounter a 'molecular traffic jam' in conventional micropores. This review differentiates itself from existing literature by focusing on the recent development of precisely engineered catalytic systems from 2020 to 2026, combining fundamental kinetics with cutting-edge technological advances. Our primary aim is to explore future directions: moving toward integrating zeolites into membrane-reactor systems that can exceed thermodynamic equilibrium limits by continuously removing water, ultimately paving the way for fully sustainable chemical production. Additionally, a key goal is to assess how embedding zeolites into membrane-reactors can surpass thermodynamic limits through ongoing water removal, offering a strategic roadmap to complete, sustainable chemical manufacturing.

Methodology for Literature Selection

To ensure a comprehensive and transparent review of the field, a systematic search strategy was employed to identify relevant studies. Literature was sourced from major academic databases, including Scopus, Web of Science, and MDPI, covering the period from 2000 to 2025.

The search was conducted using specific keywords and Boolean operators, including:

- "Zeolite-catalyzed esterification".
- "Hierarchical zeolites".
- "Solid acid catalysts AND esterification".
- "Natural zeolites AND catalytic applications".

The selection process prioritized peer-reviewed research articles and reviews that provided detailed insights into reaction mechanisms (specifically the LH and ER models), kinetic modeling, and the structural and physicochemical properties of zeolites (such as Si/Al ratio and pore size). Studies focusing on sustainable applications, such as converting biomass-derived feedstocks, such as levulinic acid or waste frying oil, into biodiesel, were given particular emphasis to align with green chemistry principles.

2. A Brief Description of Zeolites

Zeolites are hydrated aluminosilicates characterized by a framework of cavities and channels containing mobile cations and water molecules. This unique structure is the foundation of their catalytic performance in esterification, where properties such as the Si/Al ratio and pore architecture directly determine reaction efficiency. While natural zeolites like clinoptilolite are valued for their low cost and stability, their structural inconsistencies often limit their use to lower-purity applications, such as soil conditioners [41–43]. In contrast, synthetic zeolites (e.g., ZSM–5, zeolite X, β) are engineered with precise features to optimize specific industrial esterification outcomes [44–47].

2.1. Zeolite Framework and Catalytic Outcomes

The zeolite framework consists of SiO_4^{4-} and AlO_4^{5-} tetrahedra (primary building units, PBU). The link of quadrivalent silicon with trivalent aluminum creates a negative charge balanced by extra-framework cations (e.g., Na^+, Ca^{2+}) or protons (H^+), the latter of which serve as Brønsted acid sites (BAS). These sites are the primary drivers of esterification, as they protonate the carbonyl group of carboxylic acids to initiate the reaction. Representative framework structures of several typical zeolites are shown in Figure 2.

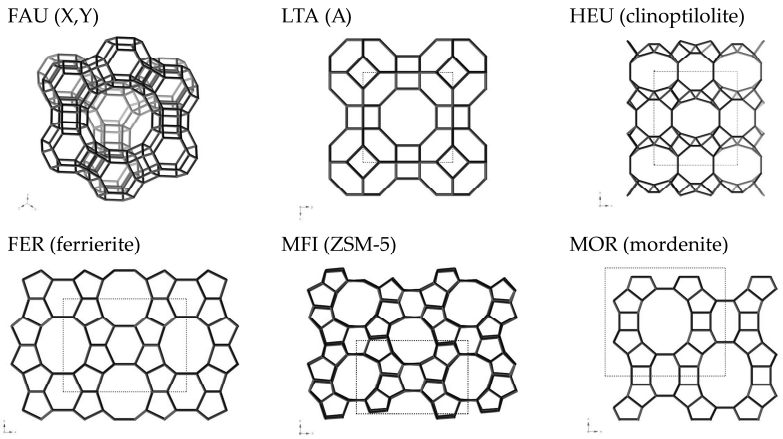

Figure 2. Representative zeolite frameworks. The three-letter codes displayed above each illustration correspond to the official framework type designations assigned by the International Zeolite Association [48], with the commonly used zeolite name provided in parentheses.

Some of the following facts shed light on the relationship that exists between structural features and the outcomes of esterification:

- The Si/Al ratio and the rates of conversion: The Si/Al ratio has an effect on the density and strength of acid sites. Additionally, a higher ratio can increase the framework's hydrophobicity, while a lower ratio typically increases the number of active sites [38,49–51]. By way of illustration, in the process of esterification of oleic acid, H–Y zeolites that have a high Si/Al ratio (80) produce significantly greater conversion rates (92%) in comparison to those that have a lower ratio of 5.2 (66%). This is because the active intermediates are stabilized more effectively [52]. The formation of rings by "Secondary Building Units" (SBU), which usually consist of eight, ten, or twelve members, creates a molecular sieving effect. Pore size also plays a crucial role in this process. This feature directly influences the selectivity of reactants by determining which molecules can access the interior catalytic sites. For example, when using a zeolite catalyst like ZSM-5 for a reaction between acetic acid and various alcohols, the narrow and uniform channels, typically about 5.5 Å in diameter, easily allow straight-chain alcohols such as *n*-butanol to ester. However, these pores are physically unable to accommodate more complex, branched molecules like 2-

ethylhexanol, which are too bulky to pass through [53,54]. This spatial restriction ensures that esterification occurs only with smaller, linear molecules, while larger molecules remain unreacted in the bulk solution. Not only does this "molecular sieving" improve selectivity, but it also prevents the formation of unwanted bulky byproducts, simplifying the overall chemical production process.

- Channel geometry and reaction kinetics: The dimensionality of the pore system, which can be either one-dimensional or three-dimensional, has a significant role in both the process of mass transfer and the production of active compounds. MFI and FER are examples of smaller 10-ring structures with lower intrinsic rate constants than BEA and MOR, which are examples of larger 12-ring structures. This is because larger 12-ring structures are more likely to promote the formation of co-adsorbed reactant complexes rather than inactive dimers. The spatial restrictions within zeolite cages, such as the FAU supercages, can stabilize specific transition states, thereby ensuring shape selectivity and product purity. It is advised that twelve-membered ring zeolites, such as Zeolite Y, be utilized in the process of glycerol esterification. This is because these zeolites can selectively form monoglycerides within their unique pore dimensions. Therefore, selecting a zeolite framework for esterification is a strategic choice that depends on the extent to which the molecular size of the ester and the internal diameter of the zeolite channel are compatible. Several physicochemical features of zeolites that have an effect on the quality of biodiesel are given in Table 1 [53–62].

Table 1. Impact of zeolite physicochemical properties on biodiesel quality.

Physicochemical Property	Effect on Catalytic Performance	Impact on Biodiesel Quality
High Si/Al Ratio	Increases framework hydrophobicity and provides better resistance to water-induced dealumination.	Longer catalyst lifespan in "wet" waste-cooking-oil feedstocks.
Strong Brønsted Acidity	Accelerates the protonation of carboxylic acids, thereby enhancing esterification rates.	Faster conversion of Free Fatty Acids (FFAs) into biodiesel.
Large Pore Diameter	Reduces steric hindrance, allowing bulky triglyceride molecules to access internal active sites.	Higher yield and reduced internal diffusion limitations.
Hierarchical Porosity	Combines micro- and mesopores to facilitate faster mass transfer of reactants and products.	Prevents catalyst "coking" and clogging during continuous flow.
High Ion-Exchange Capacity	Allows for a higher loading of alkali metals (Ca^{2+}, K^{+}, Mg^{2+} on the surface.	Increases the density of basic sites required for transesterification.

2.2. Catalytic Activity

A combination of structural and chemical features contributes to the exceptional catalytic efficiency of zeolites in the esterification process [63,64]. These structures include: (1) As shown in Figure 3, zeolites possess strong Brønsted (BAS) and Lewis acid sites (LAS), which indicate their solid acidity.

The esterification process relies on BAS, which acts as a proton donor. These proton donors are essential for activating the carboxylic acid's carboxyl group, making it more vulnerable to nucleophilic attack by the alcohol. The Si/Al ratio can be adjusted to increase or decrease the material's acidity; a lower Si/Al ratio often results in more acid sites [65–67]. Within a zeolite, the BAS serves as the central structure that facilitates esterification. It is the carbonyl oxygen (–C=O) of the carboxylic acid that is selectively protonated by these sites, which operate as proton donors. By increasing the electrophilicity of the carbonyl carbon through this protonation, the carbonyl carbon becomes much more susceptible to

nucleophilic attack by the incoming alcohol molecule. Although LAS, which are sites that accept electron pairs, are also present, the BAS is the primary factor contributing to the formation of the ester bond.

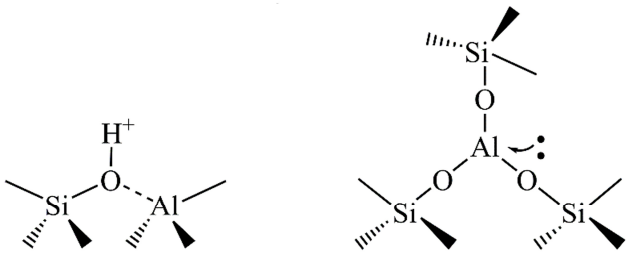

Figure 3. Illustration of BAS (left) and LAS (right) acid sites in the zeolite lattice. Replacing a Si atom in the framework with an Al atom creates BAS, which consists of bridging hydroxyl groups. LAS includes both framework and extra-framework aluminum species. These are electron-deficient centers that can accept an electron pair from a Lewis base to form a coordinate covalent bond.

(2) Form, selectivity: Zeolites have distinctive pore and channel architectures (Figure 4). As a result, the catalyst can differentiate reactant, product, and intermediate molecules based on their size and shape. Reactant selectivity ensures that only molecules small enough to enter the pores and react are involved, while product selectivity ensures that only molecules small enough to escape the pores are produced, preventing undesirable by-products [39,40,68–70]. The term "transition-state selectivity" refers to the way in which the size and configuration of zeolite pores can either stabilize or destabilize the transition state, which in turn influences the reaction pathway and selectivity.

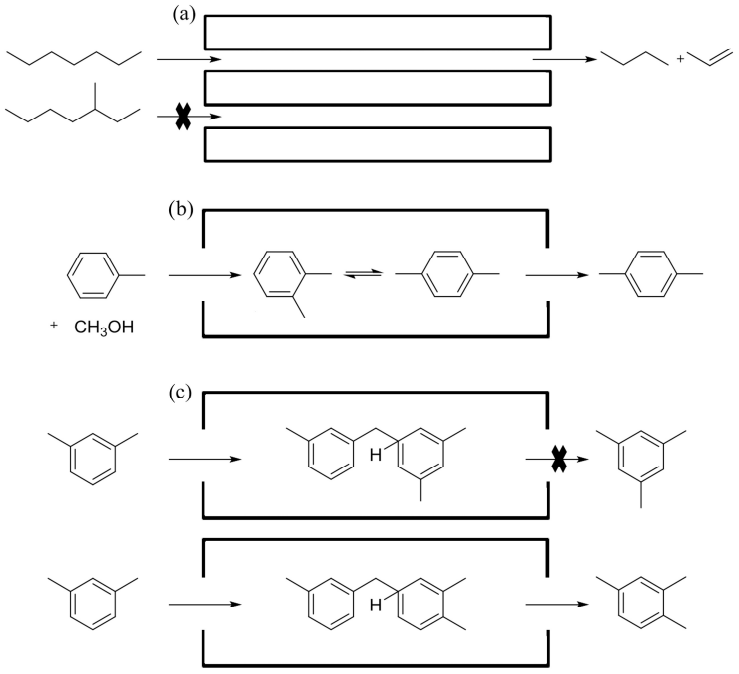

Figure 4. Shape selectivity of zeolites as solid catalysts in: (**a**) reactant selectivity during the cleavage of linear hydrocarbons, (**b**) product selectivity through the methylation of toluene, and (**c**) transition state selectivity in the disproportionation of m-xylene [71].

The catalytic performance of zeolites ZSM-5 and Y, along with montmorillonite clay K10, in glycerol esterification with free fatty acids highlights the importance of structural architecture in achieving product selectivity [72]. Although all of these materials possess acid sites, their different pore geometries act as molecular templates that favor specific

reaction pathways. The importance of pore size is best demonstrated by zeolite Y, which has a 12-membered-ring structure that provides a spacious internal environment (around 7.4 Å) that supports the transition states required for monoglyceride formation. Unlike the smaller 10-membered rings of ZSM-5, the larger cavities in zeolite Y allow bulky glycerol and fatty acid reactants to interact deeply within the pores, while also giving enough space for the resulting monoglycerides to diffuse out. This makes zeolite Y a more effective choice for producing specific partial esters compared to smaller-pore or less-structured clay options.

2.3. Acidity Tuning

The efficiency of zeolites as heterogeneous catalysts in esterification is fundamentally tied to the nature, density, strength, and accessibility of their acid sites. Because esterification requires the precise activation of a carbonyl group (C=O) by a proton donor, tuning these sites is essential to optimize catalytic activity, product selectivity, and hydrothermal stability.

In esterification, the BAS is the primary engine, providing the proton necessary to activate the carboxylic acid for nucleophilic attack by the alcohol. Primary methods for acid site optimization include: adjusting the Si/Al ratio, which is the primary lever for controlling acid site density. Low Si/Al ratio leading to a dense population of BAS. This typically increases the initial reaction rate of esterification by providing more "active workstations. A high Si/Al ratio results in lower acid density. However, this often enhances the zeolite's hydrophobicity, which is vital in esterification to prevent the water byproduct from deactivating the catalyst. In studies using H-ZSM-5 with a Si/Al ratio of ~15–25, the high Al concentration creates a dense network of BAS [73]. This leads to a very high initial conversion rate because the carboxylic acid molecules find an available proton (H^+) almost immediately upon entering the pore. Studies utilizing H-ZSM-5 with a Si/Al ratio of 100+ show a lower initial rate but much higher stability over time [74]. Because esterification produces water as a byproduct, a "crowded" low-Si/Al zeolite becomes hydrophilic; the water sticks to the acid sites, effectively "smothering" the catalyst and stopping the reaction (deactivation).

Post-synthesis dealumination removes framework Al, thereby increasing the Si/Al ratio. Although this may decrease the number of BAS, it often creates mesopores and non-framework Al species (LAS). In bulky esterification reactions involving fatty acids, these newly formed mesopores enhance accessibility, allowing larger reactants to reach previously inaccessible active sites [75–77].

Ion-exchange and isomorphic substitution can also refine the catalytic profile for esterification by replacing charge-balancing cations. Protonation (H-Form) is the standard method for maximizing the BAS required for ester bond formation. Replacing Al with atoms such as Ti, Fe, Sn, or Ga alters the acid strength [78–82]. For instance, framework metal sites can act as strong Lewis acids, selectively polarizing the carbonyl group of fatty acids and increasing their reactivity.

Standard zeolites modified with sulfated oxides (e.g., SO_4^{2-}/ZrO_2 or SO_4^{2-}/SnO_2) exhibit the highest acid strength, often called superacidity. The interaction between sulfate groups and the metal surface creates exceptionally strong acid sites [83,84]. Catalysts prepared with chlorosulfonic acid show 2–7 times higher activity in fatty acid esterification than those made with sulfuric acid, due to higher sulfur loading and larger pore sizes [85].

The bidentate binding mode of the sulfate group (Figure 5) is essential; it provides the electronic induction required for high esterification conversion. While these catalysts work well for primary alcohols, the reaction rate for secondary or tertiary alcohols (like isopropanol) is often limited by steric hindrance and polar effects at the catalyst surface [86,87].

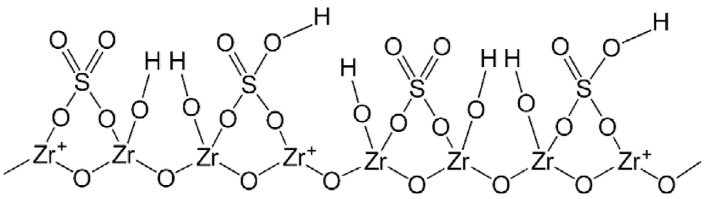

Figure 5. Suggested bidentate binding of the sulfate group on SO_4–ZrO_2 [87].

However, in esterification, sulfated oxides deactivate quickly during use due to poisoning of active sites by coke (carbonaceous deposits) [88], or they gradually leach from the metal oxide surface in liquid-phase processes, especially those involving water (e.g., esterification) or polar solvents (e.g., methanol). Strong acid sites are irreversibly lost when sulfate groups are removed, leading to a significant decline in catalytic activity over multiple cycles [88].

Zeolite support appears to help overcome some drawbacks of pure sulfated metal oxides, especially regarding stability and mass transfer. When levulinic acid (LA) was esterified to levulinates, catalysts made from cheap natural zeolite clinoptilolite and from SnO_2 or sulfated SnO_2 showed strong catalytic activity [37]. The activity of non-sulfated samples in producing octyl levulinate was about 55% and remained largely unchanged. The reason the Sn concentration had no effect was that the long octanol chains could not access the acid sites inside the catalysts' pores. Due to the high levels of LAS and BAS, sulfated SnO_2–containing clinoptilolite samples achieved complete conversion of LA to levulinates. The leaching of sulfate groups from the catalyst was kept in check by the clinoptilolite lattice structure, as evidenced by consistent activity across multiple reaction cycles. Because more coke forms during the esterification of LA to octyl levulinate than to ethyl levulinate, the sulfated catalysts exhibit higher activity in this process [37].

Measurement of Zeolite Acidity

The evaluation of acid sites (BAS and LAS) in zeolites involves several techniques for measuring acidity. Key methods include adsorption experiments with basic molecules like pyridine or ammonia for characterization. Temperature-programmed desorption (TPD), particularly NH_3–TPD, is the primary technique for measuring desorbed gases and relating them to acidity levels and strength, as indicated by desorption temperatures [89–91]. Infrared spectroscopy distinguishes between acid site types by analyzing the vibrations of probe molecules (usually pyridine), revealing protonation at Brønsted sites and providing quantitative data via vibrational frequencies [89,92–94]. Solid-state NMR offers direct insights into proton signals associated with Brønsted acid sites and the chemical environment of atoms [95–97]. Other methods, though less common, include Hammett's indicator titration and microcalorimetry for measuring the heat released during base adsorption. Therefore, the acidity of zeolite catalysts cannot be precisely determined using Hammett titration. In particular, pore confinement and acidic distribution can both strongly influence the apparent acidity of porous catalytic materials, making protonation of the Hammett indicator not the only way to evaluate zeolite acidity [98,99].

2.4. Pore Engineering, Hierarchy, and Overcoming of Diffusion Barrier

Conventional zeolites are entirely microporous, with pores smaller than 2 nm. This structure offers excellent acidity and shape selectivity but can cause slow reaction rates when bulky reactants or products, such as long-chain fatty acids or esters, are involved. A common approach to reduce diffusion limitations is to add secondary mesopores (2–50 nm) and/or macropores (>50 nm) within the micropore system, creating hierarchical zeolites with multiple levels of porosity. However, although developing hierarchical zeolite-based

catalysts helps produce more effective catalysts for complex systems, challenges and research opportunities still exist [44,100–104]. A key challenge is to introduce secondary mesopores without significantly reducing the zeolite's intrinsic micropore volume or its overall crystallinity. High crystallinity is vital for thermal/hydrothermal stability and acid strength, while maintaining micropores preserves shape selectivity. The shift from conventional to hierarchical zeolites is not simply a minor enhancement but an analytical imperative for addressing the "diffusion bottleneck" associated with LCFA esterification. Conventional zeolites (micropores < 2 nm) provide enhanced acid density and shape selectivity; however, they present significant internal mass-transfer constraints when handling bulky reactants. This results in a "molecular traffic jam," wherein the reaction rate is dictated by the velocity of molecule transit rather than the inherent chemical activity of the BAS acid sites. To address this issue, hierarchical engineering incorporates secondary mesopores (2–50 nm) or macropores (>50 nm) that function as "molecular highways". The analytical benefits of this arrangement are twofold: (1) Decoupling Diffusion from Activity: By reducing the diffusion path length, reactants access internal active sites more swiftly, allowing products to escape prior to the occurrence of secondary reactions. This is especially crucial for LCFAs, since bulky chains would otherwise obstruct exclusively microporous structures, (2) Stability through Carbon Management: Accelerated diffusion alleviates the trapping of substantial, carbon-laden intermediates, thereby diminishing "coking," which is the principal factor in catalyst deactivation inside intricate esterification systems.

An illustrative analytical case is the alteration of zeolite H- with Zr(IV) ions [105]. The resultant catalyst illustrates the direct correlation between pore engineering and industrial results:

1. Transport Efficiency: The prevalence of mesopores enhanced the transport of bulky tributyl citrate (TBC), resulting in an 80% conversion rate with complete selectivity.
2. Strategic Site Tuning: This approach facilitates the concurrent improvement of LAS while preserving the structural integrity essential for hydrothermal stability.

The primary challenge is a strategic trade-off: the introduction of mesoporosity must be meticulously regulated to prevent substantial reductions in micropore volume or overall crystallinity, both of which are crucial for preserving the high acid strength and shape selectivity that render zeolites superior to alternative solid acids.

The presence of mesopores significantly enhances catalysis in various industrial processes using zeolite-based catalysts, including heavy oil cracking with zeolite Y, the production of cumene, the hydroisomerization of alkanes over mordenite, and the synthesis of fine chemicals over Y, ZSM–5, and other zeolites [77,106–108]. Mesopores improve accessibility and transport of reactants and products, while zeolite micropores provide shape-selective properties.

Monolithic zeolite structures present a promising approach due to their high efficiency, easy recovery, and minimal catalyst loss. A new method for creating self-standing zeolite foams with a hierarchical pore structure (micro-, meso-, and macro-pores) was reported [109]. Compared to traditional catalysts that use binders, these monoliths can function as more effective catalysts. Ice-templating was used to produce sulfonated hierarchical ZSM–5 monoliths, which were then further modified. Hierarchical zeolite monoliths with sulfonic acid groups exhibited higher acid site density, improved mass transfer, and increased overall catalytic efficiency. These materials are well-suited for potential industrial applications, especially in processes such as biodiesel synthesis and oleic acid esterification, since the monolithic shape of the catalyst also simplifies recovery and reduces catalyst loss [110].

Pore engineering, which precisely controls the size and shape of micropores, is essential for achieving shape selectivity and increasing reaction rates. Improved mass transfer

(diffusion) through hierarchical structures enhances both activity and stability. Meanwhile, esterification selectivity depends on exact pore engineering within the micropores [111]. However, hierarchically structured or mesoporous zeolites are sometimes less active than regular zeolites or show no increased activity at all. Changes in zeolite porosity have led to the degradation of the original material, including weaker acidity, reduced crystallinity, and altered ion-exchange properties. The increased acidity of mesoporous zeolites may explain why the catalyst deactivates faster [112]. While these structural modifications address mass-transfer issues, they also fundamentally influence reaction kinetics, as discussed in the following section.

2.5. Surface Passivation for Adjustment of Acidity

A key factor in the catalytic efficiency of zeolites is the distribution of acid sites between the internal channels and the external crystal surface. Internal sites use shape selectivity to control which esters form inside the pores but often face significant mass transfer limitations. Meanwhile, strong acid sites on the external surface—although they lack size selectivity—provide immediate access to bulky reactants that cannot enter the micropores. Neutralization and the core–shell concept are frequently used to passivate surface acidity to prevent non-selective reactions on the crystal exterior, such as chemical vapor or liquid deposition of silicates. However, a more advanced approach involves the "core–shell" concept, where a material is engineered with a distinct inner core and an outer shell [113–116]. This architecture allows for precise control over the acid site ratio and the synergistic interaction between BAS and LAS acid sites. These composites are generally classified as zeolite@zeolite or metal-oxide@zeolite, depending on the core material.

Recent synthesis of zeolitic core–shell composites has enabled the creation of gradient acid distributions or the neutralization of unwanted surface sites [116,117]. For example, a core–shell catalyst such as mZSM–5@SO_4^{2-}/mSiO_2 utilizes a zeolite core to reduce the diffusion path length, facilitating the transport of reactants to active sites. In esterification-related pathways, such as the production of furfural from xylose, a mesoporous silica shell provides a high density of hydroxyl groups for sulfonic acid functionalization. By adjusting the quantity of SO_4^{2-}, it is possible to fine-tune the ideal BAS/LAS ratio, which is the primary driver for activating carbonyl groups and facilitating nucleophilic attack.

Despite the benefits of passivation, external acid sites are often crucial for specific esterification and etherification processes. In the production of polyoxymethylene dimethyl ethers (POMs) using H-ZSM-5, passivating the external surface has been shown to drastically limit the reaction rate. This occurs because the bulky reactants and products face severe internal diffusion restrictions within the narrow micropores. In such cases, the external acid sites contribute more significantly to the overall reaction rate than the internal ones. Introducing an intercrystalline network of mesopores has been effective; it enhances accessibility and allows a larger portion of the esterification to occur within the stabilized environment of the zeolite framework without the penalty of diffusion lag [118].

3. Mechanistic Insights and Kinetic Modeling

The overall process of esterification on acidic zeolites is similar to that of homogeneous acid catalysis, but it occurs on the solid surface and within the pores of the protonated zeolite lattice. The reaction generally takes place through several steps [39,53,119–121].

1. Adsorption of carboxylic acid and alcohol molecules, which adhere to the surface of the zeolite's internal pores.
2. Protonation of the zeolite forms BAS (proton donors). These sites protonate the carbonyl oxygen of the carboxylic acid, activating it for the reaction.

3. Nucleophilic attack occurs when alcohol acts as a nucleophile. It targets the electrophilic carbonyl carbon of the protonated carboxylic acid.
4. Proton transfer can happen either within a molecule or between molecules, resulting in a tetrahedral intermediate.
5. Dehydration happens when a water molecule is removed from the intermediate, followed by a proton release, which is then re-absorbed by the catalyst.
6. Product desorption is the last step where ester and water molecules detach from the catalyst surface, freeing active sites for another catalytic cycle.

The heterogeneous esterification process using porous catalysts involves both mass transfer and surface reactions. First, reactants diffuse through the external boundary layer, then enter the porous catalyst via pore diffusion. Inside, molecules adsorb onto active sites where esterification takes place, then desorb and return to the reaction mixture. Reactivity mainly depends on chemisorption at active sites, with adsorption occurring either associatively or dissociatively.

The two classical reaction models, the Langmuir–Hinshelwood (LH) and Eley–Rideal (ER) models, illustrate reaction kinetics (Figure 6). The first involves adsorption of both reactants on the catalyst surface, while the second involves adsorption of one reactant and a direct reaction from the bulk phase. However, experimentally validating these models is difficult, and they should be viewed as theoretical frameworks for qualitative understanding [19].

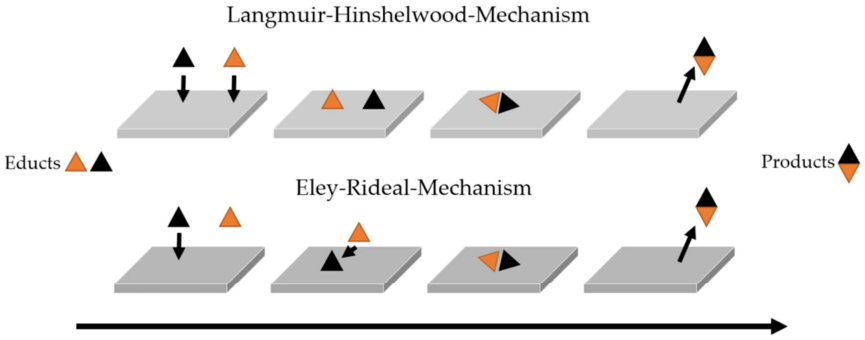

Figure 6. The Langmuir–Hinshelwood and Eley–Rideal mechanisms in heterogeneous catalysis are illustrated schematically. The formation of a black–orange product results from a reaction between a black triangle (reactant) and an orange triangle (reactant) in both cases [19].

Although they are simplified models, the LH and ER models both act as important starting points for kinetic analysis. These pathways often compete during catalytic reactions, and the preferred route can be heavily influenced by the zeolite's structure, temperature, and reactant partial pressures. Moreover, these two models describe different ways in which reactants interact with the catalyst surface:

LH Model: This mechanism assumes that both the carboxylic acid and the alcohol must be adsorbed onto adjacent active sites on the zeolite surface before the reaction occurs. The rate-determining step is typically the surface reaction between these two adsorbed species. It is often the preferred model for describing esterification in zeolites because the microporous structure promotes the simultaneous adsorption and proximity of both reactants.

ER Model: In this model, only one reactant (typically the carboxylic acid) is adsorbed and activated by the zeolite's BAS. The reaction occurs when a non-adsorbed alcohol molecule from the fluid phase directly attacks the activated, adsorbed carboxylic acid. This model may be more applicable in systems where one reactant has a significantly higher affinity for the catalyst surface than the other, or where large molecular sizes limit the

simultaneous adsorption of both species within the pores. In Table 2, the key differences of these two models are presented.

More advanced methods are needed to go beyond simplified assumptions and spatial constraints. For example, the Langmuir–Hinshelwood–Hougen–Watson (LHHW) model includes rate-limiting steps such as adsorption, surface reactions, and desorption within extended versions of the basic LH framework [122]. Microkinetic modeling involves creating a detailed kinetic model that explicitly considers all relevant intermediates and their site ensembles using simple steps and first-principles calculations, similar to Density Functional Theory (DFT) [123]. This approach provides a more accurate representation of configurational non-idealities, including coverage-dependent kinetics and non-random spatial distributions. Since kinetic parameters obtained by fitting experimental data to simplified LH or ER models may lack physical significance and only serve as curve-fitting parameters under specific experimental conditions, it is important to acknowledge their limitations.

Table 2. The key differences of LH and ER kinetic models.

Catalyst	Reactants	Kinetic Models (LH and ER)	Activation Energy, *Ea*	Findings	Reference
USY Zeolite	Oleic acid, Methyl acetate	Both LH and ER provide a good fit to the experimental results.	*Ea*: 41.77 kJ mol^{-1} Entropy variation: $\Delta S = -129.8$ J mol^{-1} K^{-1}	USY zeolite significantly reduced *Ea* compared to the uncatalyzed reaction.	[124]
ZSM−5	Liquid water phase, Methanol	LH accurately describes the kinetics.	Reaction entropy: 106.56 J K^{-1} Reaction enthalpy: 31.20 kJ mol^{-1}	Optimal conditions: 100 °C, 5 wt% ZSM-5, 89% acid conversion, 92% ester selectivity.	[125]
Hβ, HY and HZSM-5	C_3–C_4 alcohols, Acetic acid	The reaction proceeds via the ER mechanism.	–	The degree of esterification depends on the type of alcohol and the acidity of the zeolite. Zeolite Hβ was found to be the most active for this reaction.	[53]
Microporous zeolites: BEA type Beta zeolite and MFI type ZSM-5 zeolite and micro-mesoporous zeolites (MFI type ZRP-5 zeolite)	Oleic acid, Ethanol	The ER model provides a better fit to the experimental data than the LH model.	–	Zeolites with high Si/Al ratio had better catalytic performance, and of these three zeolites at the same Si/Al ratios, the ZRP-5 zeolite exhibited the lowest internal mass transfer limitations but the worst catalytic performance.	[62]
Phosphomolybdic acid supported on ZSM-5	Levulinic acid, 1-butanol	The kinetics follow a pseudo-first-order model, while the reaction mechanism is best described by an ER-1 model.	*Ea*: 79.3 kJ mol^{-1}, indicating that the reaction is kinetically controlled. The thermodynamic parameters: enthalpy of activation (76.83 kJ mol^{-1}), entropy of activation (−197.42 J. $mol^{-1} \cdot K^{-1}$), and Gibbs free energy of activation (151.45 kJ mol^{-1}), obtained from the Eyring plot.	ER mechanistic model, combined with nucleophilic acyl substitution reaction was found to best fit the experimental data.	[126]
Hβ, HY and HZSM5	Benzyl alcohol Acetic acid	The reaction follows the ER mechanism.	Hβ: 33.49 kJ mol^{-1} HY: 45.11 kJ mol^{-1} HZSM5: 40.84 kJ mol^{-1} Control: 57 kJ mol^{-1}	The esterification is controlled by acidic sites predominantly located inside the pores and the pore structure influences product selectivity.	[127]
H-Beta zeolite	Levulinic acid, Methanol	The reaction follows both LH and ER pathways.	–	Similar *Ea* suggests that both mechanisms are favorable, depending on the initial adsorption of levulinic acid and methanol.	[121]
HY zeolite	Oleic acid, Ethanol	The reaction follows the LH mechanism.	*Ea*: 41.84–52.03 kJ mol^{-1}	Thiele modulus calculations show no mass-transfer limitations within the catalyst pores.	[128]
BEA zeolite	1-octanol, Hexanoic acid	The reaction proceeds via the LH mechanism.	–	Water adsorption strongly affects esterification kinetics, being 38 times stronger than 1-octanol, while hexanoic acid, ester, and ether adsorption are negligible.	[129]

Various kinetic models, including the simple power law model, mechanism-based models of nucleophilic substitution, and LH and ER kinetics models, were examined for the selective esterification of glycerol with lauric acid using post-impregnated 12-tungstophosphoric acid SBA–15 [130]. The most accurate and reliable model combines a nucleophilic substitution mechanism with the LH kinetics model. The reaction mechanism, illustrating the process from the bulk to the molecular level of reactants and their interactions on the catalyst surface, is shown in Figure 7 [130].

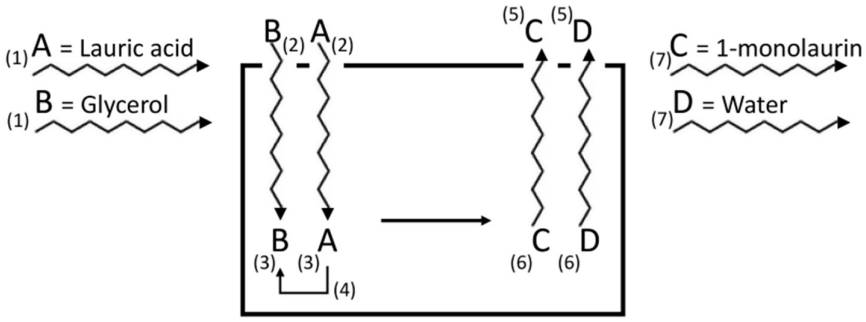

Figure 7. Mechanism of esterification of glycerol with lauric acid using a modified SBA–15. (1) External diffusion of lauric acid and glycerol takes place from the bulk fluid to the surface of the zeolite. (2) Internally, they diffuse into the mesopores. (3) Lauric acid is adsorbed and activated by acid sites on SBA–15, while glycerol adsorbs weakly. (4) A surface reaction between them produces esters and water, which are then desorbed, regenerating vacant acid sites (5). (6) Both products then diffuse internally to the external surface, leading to their diffusion back into the bulk fluid (7) [130].

The esterification of furfural to a levulinic ester, commonly called the domino reaction, involves a series of catalytic steps (Figure 8) [131]. These steps include hydrogenation, hydrolysis, ring opening, and lactonization, all facilitated by LAS and BAS. Hierarchical mordenites and zeolites, synthesized from commercial zeolites through post-synthesis techniques such as desilication or dealumination, serve as catalysts in this process. Under acidic or alkaline conditions, the improved performance of chemically treated zeolites can be attributed to the formation of larger mesopores and the creation of new acid sites, including Lewis acid sites [123].

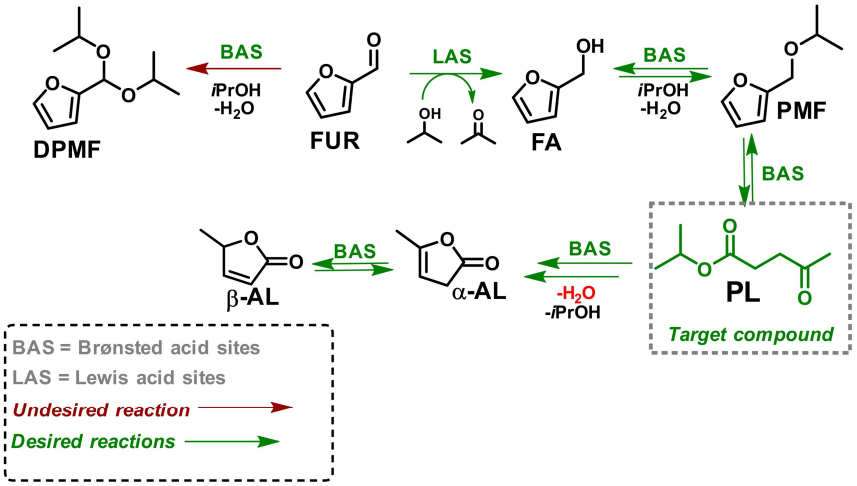

Figure 8. Schematic representation of the domino reaction: catalytic conversion of furfural to isopropyl levulinate. DPMF: 2-(diisopropoxymethyl)furan, FUR: furfural, FA: furfuryl alcohol, PMF: 2-(isopropoxymethyl)furan, PL: isopropyl levulinate, α–AL: α-angelica lactone, β–AL: β-angelica lactone. Unwanted reactions are marked in red, while desired products are displayed in green [131].

Esterification of acetic acid (AcA) with ethanol (EtOH) to produce ethyl acetate (EA), over four protonated, structurally different β–zeolites (BEA), ferrierite (FER), mordenite (MOR), and MFI (ZSM–5)—demonstrates similar effectiveness. Regardless of structural differences, an esterification mechanism is proposed involving two main surface species: an inactive ethanol dimer adsorbed on BAS, which inhibits ester formation, and a co-adsorbed complex of AcA and EtOH at the active site, which reacts to form EA (Figure 9) [119].

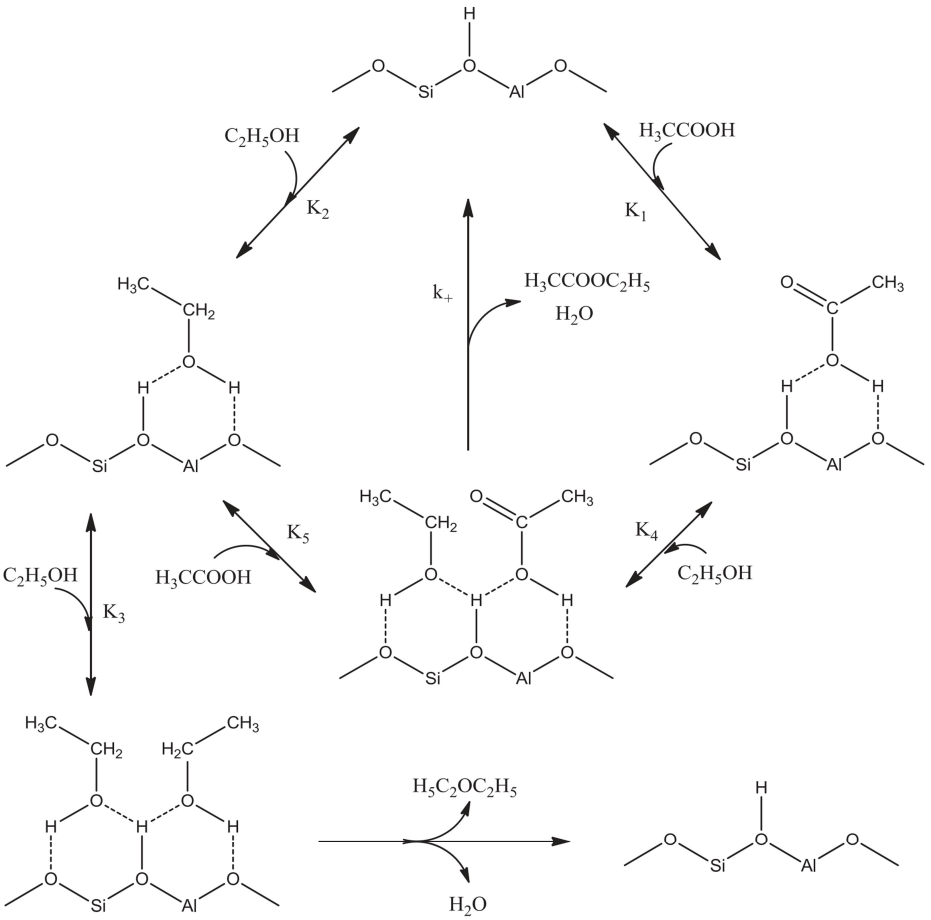

Figure 9. Reaction pathway for the esterification of acetic acid by ethanol over H–BEA, H–MFI, H–MOR, and H–FER. K_i (i:1–5) are equilibrium constants, and k_+ is the intrinsic rate constant [119].

Kinetic and thermodynamic parameters derived from this mechanism show that the intrinsic rate constant for activating the co-adsorbed complex increases in the order FER < MOR < MFI < BEA. Meanwhile, the ratio of equilibrium constants (K5/K3) increases as FER < MFI < MOR < BEA [119]. These trends can be explained by structural differences among zeolites, which vary in pore structures: BEA and MFI have 3D pore systems, whereas FER and MOR feature 1D or complex 1D/2D channel networks. MFI contains intersecting 10-ring sinusoidal and straight channels; BEA has a complex intergrowth of two 12-ring structures; MOR includes intersecting 8-ring and 12-ring channels; FER has two perpendicular intersecting channels of 8-ring and 10-ring pores. The smaller ratio of equilibrium constants for MFI and FER compared with BEA and MOR indicates that the tendency to form the co-adsorbed complex over EtOH dimers is greater on larger pore zeolites (12-membered ring) than on smaller pore zeolites (10-membered ring).

The esterification of oleic acid to methyl oleate on H–Y zeolites with different Si/Al ratios shows that this ratio is a key factor in the process. The zeolite with the highest Si/Al ratio (80) exhibited the highest esterification activity, achieving 92% conversion. This contrasts with H–Y with a Si/Al ratio of 5.2 (66% conversion), Na–Y (15% conversion),

and homogeneous acid catalysis (89% conversion) [52]. The Si/Al molar ratio affects the acidity of the active sites and hydrophobicity, both of which are crucial for esterification. A higher concentration of active sites and increased hydrophobic effects help stabilize active intermediates [132]. Theoretical calculations highlight the importance of structural features. The FAU structure (H–Y) effectively holds the oleic acid molecule during adsorption, with van der Waals interactions between the lattice walls and the aliphatic chain encouraging the integration of the large molecule into the supercages. Additionally, H–Y's higher specific surface area and greater amount of extra-framework Al species give it an advantage over H–Beta and H–ZSM–5. The combined presence of BAS and LAS within the supercages boosts the catalytic efficiency of H–Y in esterifying oleic acid (Figure 10) [52]. Furthermore, the high specific surface area of H–Y (937 m^2 g^{-1}) and the significant concentration of extra-framework Al species improve the advantages of H–Y compared to H–zeolite (634 m^2 g^{-1}) and H–ZSM–5 (509 m^2 g^{-1}). Between BAS and LAS within the supercages, a symbiotic relationship forms, boosting the catalytic effectiveness of H–Y in the esterification of oleic acid [132].

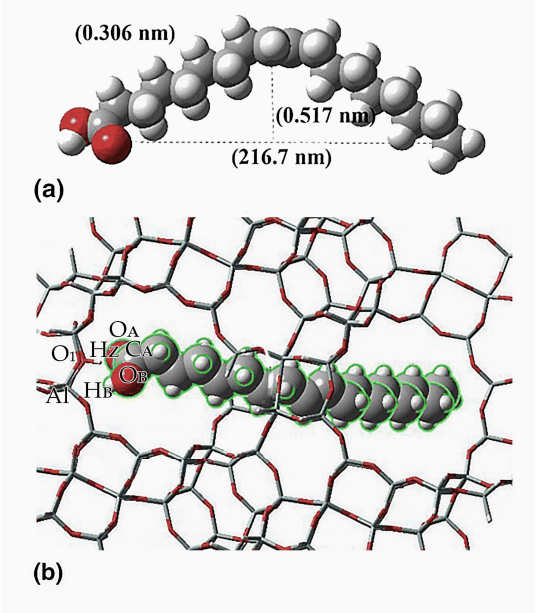

Figure 10. Interactions between oleic acid and the H–Y lattice. The dimensions of oleic acid, calculated using DFT, are shown in (**a**). The lattice features an adsorbed oleic acid molecule, illustrated in (**b**). Hydrogen atoms are white, silicon gray, oxygen red, and aluminum pink [52].

4. Process Intensification and Sustainable Applications

During zeolite-catalyzed esterification, various reactor types are used [19,133–139]. There is a strong trend toward using membrane-integrated reactors to enhance process efficiency. The most common reactors are divided into two main types: batch and continuous flow systems. Continuous-flow reactors are favored for large-scale industrial production because of their improved process control and higher throughput. Zeolites, as solid catalysts, are ideally suited for these systems. In a fixed-bed reactor, zeolite catalysts are packed into a stationary bed, with liquid reactants flowing continuously through it. This setup is also called a fixed-bed reactor. Using solid catalysts offers several advantages, including eliminating the need for a separate catalyst separation step, such as filtration, after the reaction. This allows for continuous operation. Such configurations are often used in pilot plants and ongoing commercial processes. Continuous Stirred Tank Reactors (CSTR) suspend zeolite particles within the reaction mixture. Reactants are continuously fed into the reactor, and products are constantly removed. Although it is a continuous process, it still requires

an inline solid–liquid separation device, such as a filter or centrifuge, to recover the tiny zeolite particles before the product is processed [132]. Membrane-integrated reactors are a specialized type that are especially advantageous for esterification because they overcome the limitations of thermodynamic equilibrium. An integrated selective membrane, often a zeolite membrane such as zeolite T, MOR, or AEI type, is incorporated into the reactor. This membrane allows one of the reaction products, usually water, to pass through while blocking the other components. The membrane's ability to continuously remove water as it forms shifts the reaction equilibrium toward the products (the ester and water). This significantly increases the final conversion rate beyond the typical equilibrium limit. The increased conversion rate reduces the amount of excess reactant needed, and operating temperatures and energy consumption are often lower than those of traditional methods such as reactive distillation.

Vapor-phase esterification using a zeolite membrane reactor offers advantages over traditional liquid-phase methods, notably faster reaction rates and the elimination of strong acid catalysts, such as H_2SO_4. A CHA zeolite composite membrane was developed on a porous alumina tube, demonstrating increased water vapor selectivity and permeance. Solid catalysts, including proton-exchanged zeolites CHA, FAU, USY, and H–MOR, were tested, with H–MOR showing the highest activity in vapor-phase esterification, consistent with the ER mechanism (Figure 11). A double-tube membrane reactor combining a CHA zeolite membrane and an H-mordenite catalyst enabled esterification and facilitated an equilibrium shift via selective water removal [134].

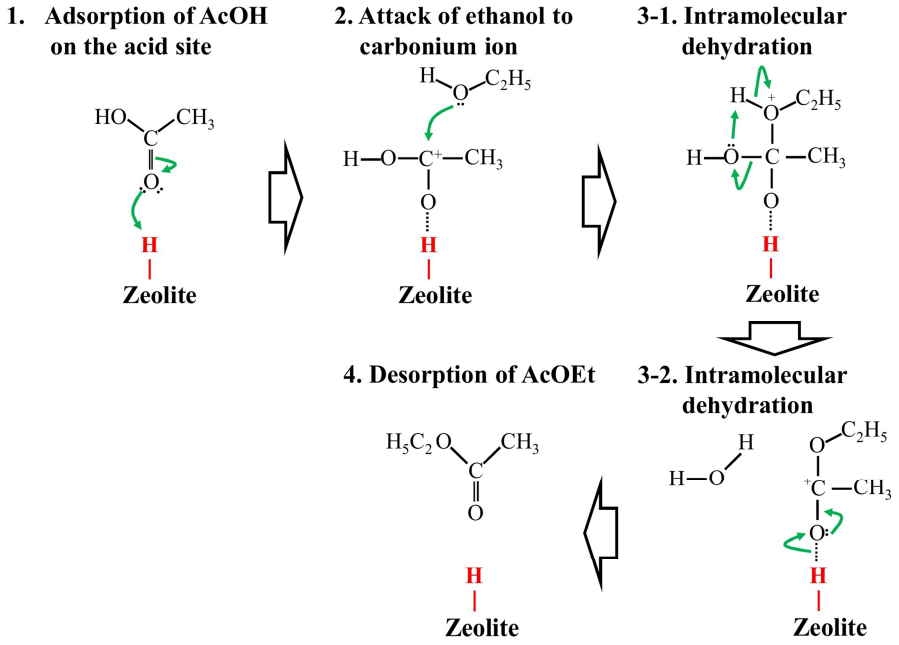

Figure 11. Esterification process by vapor phase in accordance with the Eley–Rideal mechanism [134].

More recently, a flow-type membrane reactor significantly increased the yield of ethyl acetate [135]. Using a flow-type membrane reactor with AEI-type zeolite (8-ring), the yield reached 89.0% at 363 K, surpassing the equilibrium yield of 69.1% by selectively removing water through the AEI zeolite membrane.

For membrane fabrication, 3D printing has proven to be an effective technique [140–144]. 3D printing technology is a new method for creating materials with tailored monolithic properties—such as surface area, channel size, chemical composition, and loading—that cannot be achieved through extrusion. It has been successfully used to produce adsorbent-catalyst monoliths, such as zeolites and aminosilicates (Figure 12). A series of Ga, V, and

Zr H–ZSM–5 monolithic catalysts with high metal oxide contents were prepared. The catalytic efficiency demonstrated the viability of 3D printing technology for developing highly active zeolite catalysts.

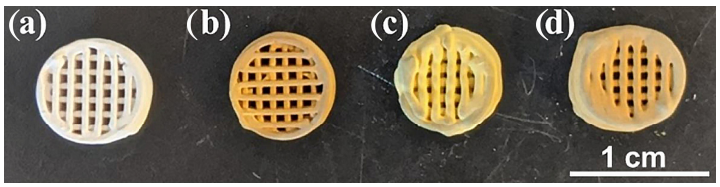

Figure 12. Photographs of (**a**) 15Ga–15Zr@ZSM–5, (**b**) 15Ga–15V@ZSM–5, (**c**) 15V–15Zr@ZSM5, and (**d**) 10Ga–10V–10Zr@ZSM–5 monoliths [140].

The sustainable use of zeolites in esterification generally follows the principles of Green Chemistry. These principles focus on using waste feedstocks, replacing hazardous reagents, and improving process efficiency. The most important and commercially relevant sustainable application is the use of zeolites to produce biodiesel (FAMEs) through the esterification of FFAs [36,55,145,146]. Low-quality feedstocks, such as animal fats and oils unsuitable for human consumption, are highly sustainable sources of biodiesel; however, they often contain high FFA levels—up to 50%. Since the base reacts with FFAs to produce soap (saponification), which consumes the catalyst, causes phase separation, and makes product purification more difficult, traditional alkaline catalysts cannot be used with oils high in FFA. Acidic zeolites like H–ZSM–5, H-Mordenite, or modified natural zeolites are very effective at catalyzing FFA esterification with methanol or ethanol to produce FAMEs. This prevents soap formation and allows the use of inexpensive waste oils. As a result, the economic and environmental benefits of biodiesel are greatly enhanced. In waste oils containing both triglycerides and FFAs, specially designed zeolite-based catalysts can be created to simultaneously esterify FFAs and transesterify triglycerides in a single reactor. These catalysts usually have both acidic and basic, or strong-acid, sites. Combining these processes in one reactor greatly simplifies the workflow, boosts efficiency, and aligns perfectly with the goals of process intensification.

4.1. Green Chemistry and Its Positive Effects on the Environment

As catalysts, powerful homogenous mineral acids, such as highly corrosive H_2SO_4, are utilized in the conventionally employed industrial esterification process. Consequently, this process requires a neutralization step that is both waste-generating and energy-intensive, resulting in the production of significant volumes of corrosive effluent and salt waste. Using straightforward filtration or centrifugation, zeolites can be easily separated from the product liquid. As a result, the neutralization stage and the associated caustic waste are eliminated, leading to a process that is far cleaner and considerably safer.

Zeolites can be recovered, regenerated (typically through a straightforward heat treatment to eliminate coke deposits), and reused for several reaction cycles This results in a significant reduction in catalyst consumption and manufacturing expenses, moving the process closer to a more circular model [147,148]. The overall chemical hazard profile of the manufacturing facility can be reduced by substituting non-toxic, recyclable solids for high-volume, harmful liquid acids.

4.2. Utilizing Waste as a Source of Catalyst

The production of zeolite-based catalysts from industrial waste materials, such as fly ash, rice husk ash, and geothermal waste, remains an active area of research [149–155]. This circular approach further promotes sustainability by converting solid waste, an environmental burden, into high-value industrial catalysts. It also helps lower catalyst costs and reduces

dependence on expensive, virgin silica and alumina sources for catalyst production. This process is known as waste valorization.

Levulinic acid is an effective esterification reagent because it is a sustainable, biomass-derived platform chemical with unique structural features that enable the synthesis of a wide range of valuable levulinate esters [156–158]. Its versatility comes from the presence of two distinct oxygen-containing functional groups: a carboxylic acid and a ketone carbonyl. It is one of the "top 12" value-added chemicals that can be efficiently and affordably produced from the acid hydrolysis of biomass. This reduces dependence on depleting, petroleum-based resources and positions it as a key chemical in future biorefineries. LA is gaining significant interest in both academia and industry to achieve economic viability through sustainable processes [159]. Esterification of LA with different alcohols using mesoporous stannosilicates as the catalyst was performed [159]. The conversion results indicated that increasing the carbon chain length significantly reduced the rate of LA conversion to esters. The shortest-chain alcohol, methanol, attained the highest conversion rate, ranging from 86.4% to 90.1%. The conversion rate of approximately 66% for butan-1-ol drops to 47.5% for sec-butanol and to 15.9% for tert-butanol, demonstrating the influence of branching in the alcohol chain on conversion efficiency. The synthesized stannosilicates exhibited both activity and stability under the evaluated reaction conditions, achieving high conversions with all primary alcohols used in this study, thereby facilitating the generation of valuable products.

Excellent effectiveness was observed for SO_4–SnO_2–clinoptilolite in converting LA to octyl and ethyl levulinate, with 100% and 70% conversion, respectively. The lower conversion to ethyl levulinate was due to coke formation during the process. Unlike long-chain octanol, short-chain ethanol easily penetrates the clinoptilolite lattice, forming coke during the esterification reaction [37]. Compared to SO_4–SnO_2, the SO_4–SnO_2–clinoptilolite catalyst is more stable, demonstrating that the clinoptilolite lattice prevents sulfate group leaching [37].

The direct esterification of FFA in waste frying oil with methanol was performed using various zeolite catalysts (ZSM–5, mordenite, faujasite, beta zeolites, and silicalite). The effectiveness of the catalysts for FFA removal decreased as the acidity in H–ZSM–5 zeolite decreased. Conversely, H-mordenite zeolites exhibited nearly the same level of FFA conversion despite differences in Si/Al molar ratios, even though their acidity was lower. The strong acid sites contributed to higher FFA conversion, while the narrow pore entrance of H–ZSM–5 zeolite enhanced FFA removal. The acidity and pore size of the zeolites influenced their catalytic activity in eliminating FFA [160].

Biodiesel is a mixture of monoalkyl esters derived from long-chain fatty acids, produced from various sources such as animal fats, vegetable oils, or waste oils through esterification and/or transesterification with alcohols, primarily methanol and ethanol. It has gained significant interest because of its low viscosity, high cetane number, high flash point, excellent lubricity, environmental benefits, and biodegradability [161,162]. Due to their ability to support both transesterification and esterification reactions, zeolites are widely studied as catalysts for biodiesel production. The activity of zeolites depends on the polarity, shape, and size of the substrate, as well as on reaction conditions. Higher reaction temperatures enhance their activity. The pore sizes of zeolites create diffusion limitations for the adsorption of triglycerides onto acid sites. Because of the lower molecular weight of FFA, zeolites perform better in esterification than in transesterification. Zeolites also tend to have fewer acid sites on their external surfaces compared to their internal surfaces, resulting in weaker acid strength, which allows large organic molecules, such as triglycerides, to react. Mesoporous zeolites, which reduce diffusion limitations, offer promising opportunities for the transesterification of vegetable oils. For example, a mesoporous silica

like SBA–15, with a high pore diameter, surface area, and pore volume, can accommodate large organic molecules. In the transesterification of diethylmalonate (DEM) with butanol, 90% conversion was achieved with 100% selectivity for DEM [163,164].

4.3. Critical Evaluation of Zeolite Performance

In biodiesel production, choosing between natural zeolites (primarily clinoptilolite) and synthetic zeolites (such as ZSM-5, X, or A) involves balancing economic sustainability and catalytic precision. In academic and pilot-scale research focused on green chemistry and cost reduction, natural zeolites are generally preferred. These minerals are mined at relatively low cost. Synthetic variants, which require high-energy hydrothermal synthesis (sometimes with expensive organic templates), are significantly more costly than natural options. Clinoptilolite is one of the most stable materials, with excellent thermal and chemical properties. Studies show it can withstand high-temperature regeneration cycles (calcination) better than some synthetic alternatives, which may lose crystallinity after multiple uses [165–169]. Additionally, natural clinoptilolite has a strong affinity for alkali and alkaline earth metals, giving it a high ion-exchange capacity. That makes it an ideal support for active basic sites, such as CaO or MgO, which are needed for the transesterification of triglycerides into biodiesel [170,171]. The life-cycle assessment (LCA) of biodiesel produced with natural zeolites generally shows a lower carbon footprint than that of biodiesel produced with synthetic catalysts [172]. This is because natural zeolites are naturally occurring and require less processing. However, natural zeolites face drawbacks related to their geological origin, lack of structural purity, and diffusion limitations (pore size < 2 nm). Because triglycerides—used as feedstocks—are large molecules, they often struggle to penetrate the narrow internal channels of natural zeolites, leading to lower yields compared to synthetic zeolites with hierarchical (meso-microporous) structures, according to research. Furthermore, natural zeolites often contain satellite minerals (quartz, clay, iron oxides) that can cause inconsistencies in catalytic performance; a sample from one region may behave differently from another. It is also common for their raw BET surface area to be lower than that of manufactured zeolites, even though they are porous. Often, activation procedures, like treatment with hydrochloric acid or sodium hydroxide, are necessary to clean and open the pores before they can be used efficiently.

Most researchers agree that raw natural zeolite is a poor catalyst on its own. However, natural zeolite that has been modified—such as CaO- or MgO-impregnated or acid-activated clinoptilolite—can achieve performance comparable to that of synthetic zeolite at a lower cost. Studies have shown, for example, that although synthetic ZSM-5 offers better shape selectivity for refining, modified clinoptilolite can reach over 95–98% biodiesel yield when properly loaded with active metal oxides [170]. This makes modified clinoptilolite the more “economically viable” option for large-scale renewable fuel production.

5. Conclusions

A crucial step toward sustainable chemical production is the transition from traditional homogeneous acid catalysis to zeolite-catalyzed esterification. This review demonstrates that zeolites are more than just alternatives; they are highly tunable platforms that can overcome the limitations of conventional methods. By shifting the industry toward waste feedstocks, such as used cooking oil rich in free fatty acids, zeolites enable a direct path to biodiesel production while preventing soap formation and eliminating energy-intensive neutralization steps.

The analytical insight provided by this study reveals that the improved performance of zeolites stems from the precise control of acid site strength and shape selectivity. However, the ‘diffusion bottleneck’—the molecular traffic jam encountered by bulky long-chain fatty

acids (LCFAs) in conventional micropores—remains the primary challenge for industrial scale-up. To address this, the field is evolving from simple catalyst comparisons to the design of highly engineered hierarchical systems. We conclude that the future of the field lies in the synergy between fundamental kinetic modeling (LH and ER models) and emerging technological tools.

Specifically, integrating Machine Learning (ML) is transforming zeolite design from a 'trial and error' process into a predictive science, enabling researchers to optimize hydrothermal synthesis and pore windows with greater precision. Additionally, additive manufacturing (3D printing) overcomes the mechanical limitations of traditional powders and pellets. By creating 3D-printed monoliths with gyroid or honeycomb structures, researchers can induce microturbulence and enhance mass transfer, ensuring effective mixing of incompatible reactants.

Ultimately, the field's aim is to move beyond the catalyst itself toward process intensification. Integrating engineered zeolites into selective membrane reactors enables continuous water removal, shifts the thermodynamic equilibrium, and allows higher conversion rates. This combination of hierarchical engineering, digital optimization, and advanced reactor design offers a comprehensive strategic roadmap to evolve zeolites into high-performance, sustainable platforms for global green chemical production.

Author Contributions: Conceptualization, N.R.; methodology, N.R.; writing—original draft preparation, N.R. and J.P.; writing—review and editing, N.R.; visualization, N.R. and J.P.; supervision, N.R. All authors have read and agreed to the published version of the manuscript.

Funding: This research was funded by the Ministry of Science, Technological Development and Innovations of the Republic of Serbia (Project number: 451-03-136/2025-03/200011).

Data Availability Statement: No new data were created or analyzed in this study. Data sharing is not applicable to this article.

Conflicts of Interest: The authors declare no conflicts of interest.

Abbreviations

The following abbreviations are used in this manuscript:

LCFA	Long-chain fatty acid
LH	Langmuir–Hinshelwood models
ER	Eley–Rideal models
FAME	Fatty acid methyl esters
PBU	Primary building units
SBU	Secondary building units
BAS	Brønsted acid sites
LAS	Lewis acid sites
LA	Levulinic acid
TPD	Temperature-programmed desorption
TBC	Tributyl citrate
POM	Polyoxymethylene dimethyl ethers
LHHW	Langmuir–Hinshelwood–Hougen–Watson
DFT	Density Functional Calculations
AcA	Acetic acid
EtOH	Ethanol
EA	Ethyl acetate
BEA	Beta zeolite
FER	Ferrierite zeolite

MOR	Mordenite zeolite
MFI	ZSM-5 zeolite
CSTR	Continuous Stirred Tank Reactors
FFA	Free fatty acids
DEM	Diethylmalonate
LCA	Life-cycle assessment
ML	Machine learning
DIW	Direct Ink Writing

References

1. Petibon, R.; Aiken, C.P.; Ma, L.; Xiong, D.; Dahn, J.R. The Use of ethyl acetate as a sole solvent in highly concentrated electrolyte for Li-ion batteries. *Electrochim. Acta* **2015**, *154*, 287–293. [CrossRef]
2. Alfano, S.; Lorini, L.; Majone, M.; Sciubba, F.; Valentino, F.; Martinelli, A. Ethylic esters as green solvents for the extraction of intracellular polyhydroxyalkanoates produced by mixed microbial culture. *Polymers* **2021**, *13*, 2789. [CrossRef] [PubMed]
3. Steele, J.H.; Bozor, M.X.; Boyce, G.R. Transmutation of scent: An evaluation of the synthesis of methyl cinnamate, a commercial fragrance, via a Fischer esterification for the second-year organic laboratory. *J. Chem. Educ.* **2020**, *97*, 4115–4121. [CrossRef]
4. Zare, M.; Golmakani, M.T.; Sardarian, A. Green synthesis of banana flavor using different catalysts: A 'study of different methods. *Green Chem. Lett. Rev.* **2020**, *13*, 83–92. [CrossRef]
5. De Nazare de Oliveira, A.; de Oliveira, D.T.; Angèlica, R.S.; de Aguiar Andrade, E.H.; do Rosàrio da Silva, J.K.; da Rocha Filo, G.N.; Coral, N.; de Oliveira Pires, L.H.; Luque, R.; Santos do Nascimento, L.A. Efficient esterification of eugenol using a microwave-activated waste kaolin. *React. Kinet. Mech. Catal.* **2020**, *130*, 633–653. [CrossRef]
6. Khan, Z.; Javed, F.; Shamair, Z.; Hafeez, A.; Fazal, T.; Aslam, A.; Zimmerman, W.B.; Rehman, F. Current developments in esterification reaction: A review on process and parameters. *J. Ind. Eng. Chem.* **2021**, *103*, 80–101. [CrossRef]
7. Ortega-Requena, S.; Montiel, C.; Máximo, F.; Gómez, M.; Murcia, M.D.; Bastida, J. Esters in the Food and Cosmetic Industries: An Overview of the Reactors Used in Their Biocatalytic Synthesis. *Materials* **2024**, *17*, 268. [CrossRef]
8. Esipovich, A.L.; Kanakov, E.A.; Charykova, T.A.; Otopkova, K.V.; Smirnov, M.A.; Mityukova, Y.A.; Belousov, A.S. A Comprehensive Study on Physicochemical Properties of Fatty Acid Esters Derived from Different Vegetable Oils and Alcohols and Their Potential Application. *Energies* **2024**, *17*, 6407. [CrossRef]
9. Lopresto, C.G.; De Paola, M.G.; De Paola, M.; Calabrò, V. Importance of the properties, collection, and storage of waste cooking oils to produce high-quality biodiesel—An overview. *Biomass Bioenergy* **2024**, *189*, 107363. [CrossRef]
10. Suhara, A.; Karyadi; Herawan, S.G.; Tirta, A.; Idris, M.; Roslan, M.F.; Putra, N.R.; Hananto, A.L.; Veza, I. Biodiesel Sustainability: Review of Progress and Challenges of Biodiesel as Sustainable Biofuel. *Clean Technol.* **2024**, *6*, 886–906. [CrossRef]
11. Olutoye, M.A.; Wong, C.P.; Chin, L.H.; Hameed, B.H. Synthesis of FAME from the methanolysis of palm fatty acid distillate using highly active solid oxide acid catalyst. *Fuel Process Technol.* **2014**, *124*, 54–60. [CrossRef]
12. Verma, P.; Sharma, M. Review of process parameters for biodiesel production from different feedstocks. *Renew. Sustain. Energy Rev.* **2016**, *62*, 1063–1071. [CrossRef]
13. Nogales-Delgado, S. Biodiesel Production and Life Cycle Assessment: Status and Prospects. *Energies* **2025**, *18*, 3338. [CrossRef]
14. Fischer, E.; Speier, A. *Berichte der Deutschen Chemischen Gesellschaft*; Verlag Chemie: Weinheim, Germany, 1895; Volume 28, pp. 3252–3258. [CrossRef]
15. Palleros, D.R. *Experimental Organic Chemistry*, 1st ed.; John Wiley & Sons: New York, NY, USA, 2000; p. 494.
16. Tian, H.; Zhao, S.; Zheng, H.; Huang, Z. Optimization of coproduction of ethyl acetate and n-butyl acetate by reactive distillation. *Chin. J. Chem. Eng.* **2015**, *23*, 667–674. [CrossRef]
17. Sato, T.; Nagasawa, H.; Kanezashi, M.; Tsuru, T. Enhanced production of butyl acetate via methanol-extracting transesterification membrane reactors using organosilica membrane: Experiment and modeling. *Chem. Eng. J.* **2022**, *429*, 132188. [CrossRef]
18. Al-Rabiah, A.A.; Alqahtani, A.E.; Al Darwish, R.K.; Bin Naqyah, A.S. Novel process for butyl acetate production via membrane reactor: A comparative study with the conventional and reactive distillation processes. *Processes* **2022**, *10*, 1801. [CrossRef]
19. Hoff, K.L.; Eisenacher, M. Process Intensification Strategies for Esterification: Kinetic Modeling, Reactor Design, and Sustainable Applications. *Int. J. Mol. Sci.* **2025**, *26*, 7214. [CrossRef]
20. Yusuf, B.O.; Oladepo, S.A.; Ganiyu, S.A. Efficient and Sustainable Biodiesel Production via Transesterification: Catalysts and Operating Conditions. *Catalysts* **2024**, *14*, 581. [CrossRef]
21. Melchiorre, M.; Cucciolito, M.E.; Di Serio, M.; Ruffo, F.; Tarallo, O.; Trifuoggi, M.; Esposito, R. Homogeneous Catalysis and Heterogeneous Recycling: A Simple Zn(II) Catalyst for Green Fatty Acid Esterification. *ACS Sustain. Chem. Eng.* **2021**, *9*, 6001–6011. [CrossRef]
22. Clark, J. Solid Acids for Green Chemistry. *Acc. Chem. Res.* **2002**, *35*, 791–797. [CrossRef]

23. Doyle, A.M.; Albayati, T.M.; Abbas, A.S.; Alismaeel, Z.T. Biodiesel production by esterification of oleic acid over zeolite Y prepared from kaolin. *Renew. Energy* **2016**, *97*, 19–23. [CrossRef]
24. Patel, A.; Brahmkhatri, V.; Singh, N. Biodiesel production by esterification of free fatty acid over sulfated zirconia. *Renew. Energy* **2013**, *51*, 227–233. [CrossRef]
25. Rezende, M.J.; Pinto, A.C. Esterification of fatty acids using acid-activated Brazilian smectite natural clay as a catalyst. *Renew. Energy* **2016**, *92*, 171–177. [CrossRef]
26. Hua, J.; Ji, M.; Jiao, P.; Yin, Z.; Xia, Q.; Jiang, L.; Zhang, J.; Pan, H. Heterogeneous acid catalysts for biodiesel production: Effect of physicochemical properties on their activity and reusability. *Catalysts* **2025**, *15*, 396. [CrossRef]
27. Zhang, H.; Tian, F.; Xu, L.; Peng, R.; Li, Y.; Deng, J. Batch and continuous esterification for the direct synthesis of high qualified biodiesel from waste cooking oils (WCO) with Amberlyst-15/Poly(vinyl alcohol) membrane as a bifunctional catalyst. *Chem. Eng. J.* **2020**, *388*, 124214. [CrossRef]
28. Salaheldeen, M.; Mariod, A.A.; Aroua, M.K.; Rahman, S.M.A.; Soudagar, M.E.M.; Fattah, I.M.R. Current state and perspectives on transesterification of triglycerides for biodiesel production. *Catalysts* **2021**, *11*, 1121. [CrossRef]
29. Ramírez, E.; Iborra, M.; Tejero, J. Catalysts: Advances in the catalytic behavior of ion-exchange resins. *Catalysts* **2024**, *14*, 704. [CrossRef]
30. Katada, N.; Endo, J.; Notsu, K.; Yasunobu, N.; Naito, N.; Niwa, M. Superacidity and catalytic activity of sulfated zirconia. *J. Phys. Chem. B* **2000**, *104*, 10321–10328. [CrossRef]
31. Wang, S.; Pu, J.; Wu, J.; Liu, H.; Xu, H.; Li, X.; Wang, H. SO_4^{2-}/ZrO_2 as a solid acid for the esterification of palmitic acid with methanol: Effects of the calcination time and recycle method. *ACS Omega* **2020**, *5*, 30139–30147. [CrossRef]
32. Sadaba, I.; López Granados, M.; Riisager, A.; Taarning, E. Deactivation of solid catalysts in liquid media: The case of leaching of active sites in biomass conversion reactions. *Green Chem.* **2015**, *17*, 4133–4145. [CrossRef]
33. Rabee, A.I.M.; Mekhemer, G.A.H.; Osatiashtiani, A.; Isaacs, M.A.; Lee, A.F.; Wilson, K.; Zaki, M.I. Acidity-reactivity relationships in catalytic esterification over ammonium sulfate-derived sulfated zirconia. *Catalysts* **2017**, *7*, 204. [CrossRef]
34. Lowe, B.; Gardy, J.; Hassanpour, A. The role of sulfated materials for biodiesel production from cheap raw materials. *Catalysts* **2022**, *12*, 223. [CrossRef]
35. Climent, M.J.; Corma, A.; Iborra, S. Heterogeneous catalysts for the one-pot synthesis of chemicals and fine chemicals. *Chem. Rev.* **2011**, *111*, 1072–1133. [CrossRef]
36. Fattahi, N.; Triantafyllidis, K.; Luque, R.; Ramazani, A. Zeolite-based catalysts: A valuable approach toward ester bond formation. *Catalysts* **2019**, *9*, 758. [CrossRef]
37. Pavlović, J.; Popova, M.; Mihalyi, R.M.; Mazaj, M.; Mali, G.; Kovač, J.; Lazarova, H.; Rajić, N. Catalytic activity of SnO_2- and SO_4/SnO_2-containing clinoptilolite in the esterification of levulinic acid. *Microporous Mesoporous Mater.* **2019**, *279*, 10–18. [CrossRef]
38. Lodhi, A.; Maheria, K.C. Zeolite-catalysed esterification of biomass-derived acids into high-value esters products: Towards sustainable chemistry. *Catal. Commun.* **2024**, *187*, 106883. [CrossRef]
39. Gomes, G.J.; Zalazar, M.F.; Padilha, J.C.; Costa, M.B.; Bazzi, C.L.; Arroyo, P.A. Unveiling the mechanisms of carboxylic acid esterification on acid zeolites for biomass-to-energy: A review of the catalytic process through experimental and computational studies. *Chemosphere* **2024**, *349*, 140879. [CrossRef]
40. Zormpa, F.; Treu, P.; Saraçi, E. Advancing biomass valorization with zeolite catalysts: Focus on oxidative transformations. *Sustain. Chem. Environ.* **2025**, *10*, 100249. [CrossRef]
41. Mondal, M.; Biswas, B.; Garai, S.; Sarkar, S.; Banerjee, H.; Brahmachari, K.; Bandyopadhyay, P.K.; Maitra, S.; Brestic, M.; Skalicky, M.; et al. Zeolites enhance soil health, crop productivity and environmental safety. *Agronomy* **2021**, *11*, 448. [CrossRef]
42. Javaid, A.; Munir, N.; Abideen, Z.; Siddiqui, Z.S.; Yong, J.W.H. The role of natural and synthetic zeolites as soil amendments for mitigating the negative impacts of abiotic stresses to improve agricultural resilience. *Plant Stress* **2024**, *14*, 100627. [CrossRef]
43. Khajeh, A.; Salimi, M.; MolaAbasi, H.; Seif, M.E.; Payan, M.; Keawsawasvong, S. Zeolite-Based Soil Stabilization: A Review. *J. Rock Mech. Geotech. Eng.* **2025**, *in press*. [CrossRef]
44. Mardiana, S.; Azhari, N.J.; Ilmi, T.; Kadja, G.T.M. Hierarchical zeolite for biomass conversion to biofuel: A Review. *Fuel* **2022**, *309*, 122119. [CrossRef]
45. Yan, P.; Wang, H.; Liao, Y.; Wang, C. Zeolite catalysts for the valorization of biomass into platform compounds and biochemicals/biofuels: A review. *Renew. Sustain. Energy Rev.* **2023**, *178*, 113219. [CrossRef]
46. Naseef, H.H.; Tulaimat, R.H. Transesterification and esterification for biodiesel production: A comprehensive review of catalysts and palm oil feedstocks. *Energy Convers. Manag. X* **2025**, *26*, 100931. [CrossRef]
47. Tian, J.; Tan, K.B.; Li, Y.; Zhan, G. Engineering hierarchical zeolites via bio-inspired routes: From synthesis to application. *Coord. Chem. Rev.* **2026**, *549*, 217349. [CrossRef]
48. Database of Zeolite Structures. Available online: https://europe.iza-structure.org/IZA-SC/ftc_table.php (accessed on 31 January 2026).

49. Kordala, N.; Wyszkowski, M. Zeolite properties, methods of synthesis, and selected applications. *Molecules* **2024**, *29*, 1069. [CrossRef]
50. Szkudlarek, Ł.; Chałupka-Śpiewak, K.; Maniukiewicz, W.; Nowosielska, M.; Szynkowska-Jóźwik, M.I.; Mierczyński, P. Biodiesel production by methanolysis of rapeseed oil—Influence of SiO_2/Al_2O_3 ratio in BEA zeolite structure on physicochemical and catalytic properties of zeolite systems with alkaline earth oxides (MgO, CaO, SrO). *Int. J. Mol. Sci.* **2024**, *25*, 3570. [CrossRef]
51. Nagaraju, N.; Kumaraswamy, K.; Kumar, S.P.; Harishekar, M.; Chirauri, S.T.; Kim, S.; Srinivasrao, G.; Putrakumar, B. Tungsten trioxide-modified zeolite-based catalysts in the esterification of lactic acid: The effect of Si/Al ratio and WO_3 loadings. *Emergent Mater.* **2023**, *6*, 1351–1362. [CrossRef]
52. Gomes, G.J.; Dal Pozzo, D.M.; Zalazar, M.F.; Costa, M.B.; Arroyo, P.A.; Bittencourt, P.R. Oleic acid esterification catalyzed by zeolite Y-model of the biomass conversion. *Top. Catal.* **2019**, *62*, 874–883. [CrossRef]
53. Kirumakki, S.R.; Nagaraju, N.; Chary, K.V.R. Esterification of alcohols with acetic acid over zeolites Hβ, HY and HZSM5. *Appl. Catal. A-Gen.* **2006**, *299*, 185–192. [CrossRef]
54. Kamonlatth Rodponthukwaji, K.; Wattanakit, C.; Yutthalekha, T.; Assavapanumat, S.; Warakulwit, C.; Wannapakdee, W.; Limtrakul, J. Catalytic upgrading of carboxylic acids as bio-oil models over hierarchical ZSM-5 obtained via an organosilane approach. *RSC Adv.* **2017**, *7*, 35581–35589. [CrossRef]
55. Yusuf, B.O.; Oladepo, S.A.; Ganiyu, S.A. Biodiesel production from waste cooking oil via *β*-zeolite-supported sulfated metal oxide catalyst systems. *ACS Omega* **2023**, *8*, 23720–23732. [CrossRef]
56. Pang, H.; Yang, G.; Li, L.; Yu, J. Efficient transesterification over two-dimensional zeolites for sustainable biodiesel production. *Green Energy Environ.* **2020**, *5*, 405–413. [CrossRef]
57. Bello, F.O.; Kagher, J.; Safiyanu, R.S.; Usman, R.A.; Abdukareem, A.S.; Kovo, A.S. Production and characterization of hierarchical zeolite Y catalyst for biodiesel production using waste cooking oil as a feedstock. *Biofuels* **2023**, *14*, 365–372. [CrossRef]
58. Fawaz, E.G.; Salam, D.A.S.; Rigolet, S.; Daou, T.J. Hierarchical zeolites as catalysts for biodiesel production from waste frying oils to overcome mass transfer limitations. *Molecules* **2021**, *26*, 4879. [CrossRef]
59. Yang, G.; Yu, J. Advancements in basic zeolites for biodiesel production via transesterification. *Chemistry* **2023**, *5*, 438–451. [CrossRef]
60. Saad, M.; Siyo, B.; Alrakkad, H. Preparation and characterization of biodiesel from waste cooking oils using heterogeneous catalyst (Cat.TS-7) based on natural zeolite. *Heliyon* **2023**, *9*, e15836. [CrossRef] [PubMed]
61. Brito, A.; Borges, M.E.; Otero, N. Zeolite Y as a heterogeneous catalyst in biodiesel fuel production from used vegetable oil. *Energy Fuels* **2007**, *21*, 3280–3283. [CrossRef]
62. Sun, K.; Lu, J.; Ma, L.; Han, Y.; Fu, Z.; Ding, J. A comparative study on the catalytic performance of different types of zeolites for biodiesel production. *Fuel* **2015**, *158*, 848–854. [CrossRef]
63. Verdoliva, V.; Saviano, M.; De Luca, S. Zeolites as acid/basic solid catalysts: Recent synthetic developments. *Catalysts* **2019**, *9*, 248. [CrossRef]
64. Haw, J.F. Zeolite acid strength and reaction mechanisms in catalysis. *Phys. Chem. Chem. Phys.* **2002**, *4*, 5431–5441. [CrossRef]
65. Silaghi, M.C.; Chizallet, C.; Raybaud, P. Challenges on molecular aspects of dealumination and desilication of zeolites. *Microporous Mesoporous Mater.* **2014**, *191*, 82–96. [CrossRef]
66. Xu, B.; Bordiga, S.; Prins, R.; van Bokhoven, J.A. Effect of framework Si/Al ratio and extra-framework aluminum on the catalytic activity of Y zeolite. *Appl. Catal. A Gen.* **2007**, *333*, 245–253. [CrossRef]
67. Li, B.; Wen, M.; Ding, Y.; Zheng, W.; Sun, W.; Zhao, L. Unveiling the enhanced catalytic performance of low-Si/Al-ratio beta-zeolite on C4 alkylation combing with experiments and molecular simulations. *Chem. Eng. Sci.* **2024**, *300*, 120609. [CrossRef]
68. Qazi, U.Y.; Javaid, R.; Ikhlaq, A.; Khoja, A.H.; Saleem, F. A Comprehensive review on zeolite chemistry for catalytic conversion of biomass/waste into green fuels. *Molecules* **2022**, *27*, 8578. [CrossRef]
69. Liu, S.; Cheng, Z.; Li, B.; Zeng, H.; Liang, W.; Luo, Y.; Bai, Y.; Gao, H.; Pan, X.; Shu, X. Recent advances in biomass-assisted synthesis of hierarchical porous zeolite. *Mater. Today Sustain.* **2024**, *27*, 100917. [CrossRef]
70. Morankar, D.; Barhate, K.; Hatvate, N. ZSM-5 Zeolite: Structural features, catalytic properties, and multidisciplinary applications in organic synthesis, material science, and environmental remediation. *Coord. Chem. Rev.* **2026**, *549*, 217245. [CrossRef]
71. Dhakshinamoorthy, A.; Garcia, H.; Asiri, A.M. Catalysis in confined spaces of metal organic frameworks. *Chem. Cat. Chem.* **2020**, *12*, 4732–4753. [CrossRef]
72. Heykants, E.; Verrelst, W.H.; Parton, R.F.; Jacobs, P.A. Shape-selective zeolite catalysed synthesis of monoglycerides by Esterification of fatty acids with glycerol. *Stud. Surf. Sci. Catal.* **1997**, *105*, 1277–1284. [CrossRef]
73. Nastase, S.A.F.; Cavallo, L. Role of acid site density and pore type on the Brønsted acid strength of zeolite H-ZSM-5. *Catal. Lett.* **2025**, *155*, 155. [CrossRef]
74. Fawaz, E.G.; Salam, D.A.; Daou, T.J. Esterification of linoleic acid using HZSM-5 zeolites with different Si/Al ratios. *Microporous Mesoporous Mater.* **2020**, *294*, 109855. [CrossRef]

75. Jia, X.; Khan, W.; Wu, Z.; Choi, J.; Yip, A.C.K. Modern synthesis strategies for hierarchical zeolites: Bottom-up versus top-down strategies. *Adv. Powder Technol.* **2019**, *30*, 467–484. [CrossRef]
76. Chal, R.; Gérardin, D.C.; Bulut, D.M.; van Dobk, D.S. Overview and industrial assessment of synthesis strategies towards zeolites with mesopores. *Chem. Cat. Chem.* **2011**, *3*, 67–81. [CrossRef]
77. van Donk, S.; Janssen, A.H.; Bitter, J.H.; de Jong, K.P. Generation, characterization, and impact of mesopores in zeolite catalysts. *Catal. Rev.* **2003**, *45*, 297–319. [CrossRef]
78. Corma, A.; Nemeth, L.; Renz, M.; Valencia, S. Sn-zeolite beta as a heterogeneous chemoselective catalyst for Baeyer–Villiger oxidations. *Nature* **2001**, *412*, 423–425. [CrossRef]
79. Han, L.; Wen, C.; Wu, Z.; Wang, J.; Chang, L.; Feng, G.; Zhang, R.; Kong, D.; Liu, J. Density functional theory investigations into the structures and acidity properties of Ti-doped SSZ-13 zeolite. *Microporous Mesoporous Mater.* **2017**, *237*, 132–139. [CrossRef]
80. Zhang, H.; Samsudin, I.B.; Jaenicke, S.; Chuah, G.-K. Zeolites in catalysis: Sustainable synthesis and its impact on properties and applications. *Catal. Sci. Technol.* **2022**, *12*, 6024–6039. [CrossRef]
81. Zhang, J.; Zakeri, T.; Yue, Q.; Kubů, M.; Barakov, R.; Přech, J.; Opanasenko, M.; Shamzhy, M. Lewis acid zeolite catalysts via chemical modification of extra-large pore germanosilicates. *Catal. Today* **2024**, *440*, 114825. [CrossRef]
82. Yang, Z.; Ge, Q.; Zhu, X. Heteroatom lewis acid zeolites: Synthesis, characterization and application in the conversion of biomass-derived oxygenates. *Green Chem.* **2024**, *26*, 8068–8099. [CrossRef]
83. Arata, K. Preparation of superacids by metal oxides for reactions of butanes and pentanes. *Appl. Catal. A-Gen.* **1996**, *146*, 3–32. [CrossRef]
84. Arata, K. Solid Superacids. *Adv. Catal.* **1990**, *37*, 165–211. [CrossRef]
85. Grecea, M.L.; Dimian, A.C.; Tanase, S.; Subbiah, V.; Rothenberg, G. Sulfated zirconia as a robust superacid catalyst for multiproduct fatty acid esterification. *Catal. Sci. Technol.* **2012**, *2*, 1500–1506. [CrossRef]
86. Sekewael, S.J.; Pratika, R.A.; Hauli, L.; Amin, A.K.; Utami, M.; Wijaya, K. Recent progress on sulfated nanozirconia as a solid aid catalyst in the hydrocracking reaction. *Catalysts* **2022**, *12*, 191. [CrossRef]
87. Wang, P.; Zhang, J.; Han, C.; Yang, C.; Li, C. Effect of modification methods on the surface properties and *n*-butane isomerization performance of La/Ni-promoted SO_4^{2-}/ZrO_2-Al_2O_3. *Appl. Surf. Sci.* **2016**, *378*, 489–495. [CrossRef]
88. Yan, G.X.; Wang, A.; Wachs, I.E.; Baltrusaitis, J. Critical review on the active site structure of sulfated zirconia catalysts and prospects in fuel production. *Appl. Catal. A-Gen.* **2019**, *572*, 210–225. [CrossRef]
89. Lok, B.M.; Marcus, B.K.; Angell, C.L. Characterization of zeolite acidity. II. Measurement of zeolite acidity by ammonia temperature programmed desorption and FTIR spectroscopy techniques. *Zeolites* **1986**, *6*, 185–194. [CrossRef]
90. Niwa, M.; Katada, N. Measurements of acidic property of zeolites by temperature programmed desorption of ammonia. *Catal. Surv. Asia* **1997**, *1*, 215–226. [CrossRef]
91. Rodríguez-González, L.; Hermes, F.; Bertmer, M.; Rodríguez-Castellón, E.; Jiménez-López, A.; Simon, U. The acid properties of H-ZSM-5 as studied by NH_3-TPD and ^{27}Al-MAS-NMR spectroscopy. *Appl. Catal. A Gen.* **2007**, *328*, 174–182. [CrossRef]
92. Jin, F.; Li, Y. A FTIR and TPD examination of the distributive properties of acid sites on ZSM-5 zeolite with pyridine as a probe molecule. *Catal. Today* **2009**, *145*, 101–107. [CrossRef]
93. Zholobenko, V.; Freitas, C.; Jendrlin, M.; Bazin, P.; Travert, A.; Hibault-Starzyk, F. Probing the acid sites of zeolites with pyridine: Quantitative AGIR measurements of the molar absorption coefficients. *J. Catal.* **2020**, *385*, 52–60. [CrossRef]
94. Dalena, F.; Dib, E.; Onida, B.; Ferrarelli, G.; Daturi, M.; Giordano, G.; Migliori, M.; Mintova, S. Evaluation of zeolite composites by IR and NMR spectroscopy. *Molecules* **2024**, *29*, 4450. [CrossRef] [PubMed]
95. Gilson, J.-P.; Fernandez, C.; Thibault-Starzyk, F. New insights on zeolite chemistry by advanced IR and NMR characterization tools. *J. Mol. Catal. A Chem.* **2009**, *305*, 54–59. [CrossRef]
96. Li, S.; Zhou, L.; Zheng, A.; Deng, F. Recent advances in solid state NMR characterization of zeolites. *Chin. J. Catal.* **2015**, *36*, 789–796. [CrossRef]
97. Zachariou, A.; Hawkins, A.P.; Howe, R.F.; Skakle, J.M.S.; Barrow, N.; Collier, P.; Nye, D.W.; Smith, R.I.; Stenning, G.B.G.; Parker, S.F.; et al. Counting the acid sites in a commercial ZSM-5 zeolite catalyst. *ACS Phys. Chem. Au* **2023**, *3*, 74–83. [CrossRef]
98. Derouane, E.G.; Védrine, J.C.; Pinto, R.R.; Borges, P.M.; Costa, L.; Lemos, M.A.N.D.A.; Lemos, F.; Ribeiro, F.R. The acidity of zeolites: Concepts, measurements and relation to catalysis: A review on experimental and theoretical methods for the study of zeolite acidity. *Catal. Rev.* **2013**, *55*, 454–515. [CrossRef]
99. Chen, W.; Yi, X.; Huang, L.; Liu, W.; Li, G.; Acharya, D.; Sun, X.; Zheng, A. Can Hammett indicators accurately measure the acidity of zeolite catalysts with confined space? Insights into the mechanism of coloration. *Catal. Sci. Technol.* **2019**, *9*, 5045–5057. [CrossRef]
100. Verboekend, D.; Pérez-Ramírez, J. Design of hierarchical zeolitecatalysts by desilication. *Catal. Sci. Technol.* **2011**, *1*, 879–890. [CrossRef]
101. Khan, W.; Jia, X.; Wu, Z.; Choi, J.; Yip, A.C.K. Incorporating hierarchy into conventional zeolites for catalytic biomass conversions: A review. *Catalysts* **2019**, *9*, 127. [CrossRef]

102. Oliveira, D.S.; Lima, R.B.; Pergher, S.B.C.; Caldeira, V.P.S. Hierarchical zeolite synthesis by alkaline treatment: Aadvantages and applications. *Catalysts* **2023**, *13*, 316. [CrossRef]
103. Wei, Y.; Feng, J.; Guan, B.; Yu, J. Structural engineering of hierarchical zeolite-based catalysts. *Acc. Mater. Res.* **2024**, *5*, 857–871. [CrossRef]
104. Zieliński, M.; Matysiak, N.; Janiszewska, E. Rational design of hierarchical Beta zeolites via post-synthesis treatments and their applications. *Molecules* **2025**, *30*, 1030. [CrossRef]
105. Li, H.; Zhao, S.; Zhang, W.; Du, H.; Yang, X.; Peng, Y.; Han, D.; Wang, B.; Li, Z. Efficient esterification over hierarchical Zr-Beta zeolite synthesized via liquid-state ion-exchange strategy. *Fuel* **2023**, *342*, 127786. [CrossRef]
106. Konnov, S.V.; Ivanova, I.I.; Ponomareva, O.A.; Zaikovskii, V.I. Hydroisomerization of n-alkanes over Pt-modified micro/mesoporous materials obtained by mordenite recrystallization. *Microporous Mesoporous Mater.* **2012**, *164*, 222–231. [CrossRef]
107. Jin, J.; Peng, C.; Wang, J.; Liu, H.; Gao, X.; Liu, H.; Xu, C. Facile synthesis of mesoporous zeolite Y with improved catalytic performance for heavy oil fluid catalytic cracking. *Ind. Eng. Chem. Res.* **2014**, *53*, 3406–3411. [CrossRef]
108. Liu, Y.; Zou, Y.; Jiang, H.; Gao, H.; Chen, R. Deactivation mechanism of beta-zeolite catalyst for synthesis of cumene by benzene alkylation with isopropanol. *Chin. J. Chem. Eng.* **2017**, *25*, 1195–1201. [CrossRef]
109. Chen, J.; Liu, F.; Li, Y.; Dou, Y.; Liu, S.; Xiao, L. Self-standing zeolite foam monoliths with hierarchical micro-meso-macroporous structures. *R. Soc. Open Sci.* **2020**, *7*, 200981. [CrossRef]
110. Zhao, B.; Yang, P.; Zhang, N.; Inns, D.R.; Kozhevnikova, E.F.; Katsoulidis, A.P.; Kozhevnikov, I.V.; Steiner, A.; Zhang, H. Sulfonated hierarchical ZSM-5 zeolite monoliths as solid acid catalyst for esterification of oleic acid. *Chem. Commun.* **2024**, *60*, 13356–13359. [CrossRef]
111. Nikoshvili, L.Z.; Bronstein, L.M.; Matveeva, V.G.; Sulman, M.G. Enhancing the catalytic performance of zeolites via metal doping and porosity control. *Molecules* **2025**, *30*, 3798. [CrossRef]
112. Rutkowska, M.; Chmielarz, L. Application of mesoporous/hierarchical zeolites as catalysts for the conversion of nitrogen pollutants: A review. *Catalysts* **2024**, *14*, 290. [CrossRef]
113. Kosinov, N.; Liu, C.; Hensen, E.J.M.; Pidko, E.A. Engineering of transition metal catalysts confined in zeolites. *Chem. Mater.* **2018**, *30*, 3177–3198. [CrossRef] [PubMed]
114. Le, T.T.; Shilpa, K.; Lee, C.; Han, S.; Weiland, C.; Bare, S.R.; Dauenhauer, P.J.; Rimer, J.D. Core-shell and egg-shell zeolite catalysts for enhanced hydrocarbon processing. *J. Catal.* **2022**, *405*, 664–675. [CrossRef]
115. Wang, W.; He, L.; Luo, Q.; Wang, L.; Wang, J.; Chen, H.; Miao, Z.; Yao, Q.; Sun, M. Synthesis and application of core-shell, hollow, yolk-shell multifunctional structure zeolites. *Microporous Mesoporous Mater.* **2023**, *362*, 112766. [CrossRef]
116. Ferrarelli, G.; Migliori, M.; Catizzone, E. Recent trends in tailoring external acidity in zeolites for catalysis. *ACS Omega* **2024**, *9*, 29072–29087. [CrossRef]
117. Ji, R.; Yin, D.; Chen, Y.; Ma, L.; Lv, F.; Zhang, Y.; Jia, Z.; Zhang, J.; Liu, M.; Yu, S.; et al. Efficient synthesis of furfural over mZSM-5@SO_4^{2-}/mSiO_2 core–shell catalyst by targeted regulating B/L acids. *Fuel* **2024**, *363*, 130907. [CrossRef]
118. Baranowski, C.J.; Bahmanpour, A.M.; Héroguel, F.; Luterbacher, J.S.; Kröcher, O. Prominent role of mesopore surface area and external acid sites for the synthesis of polyoxymethylene dimethyl ethers (OME) on a hierarchical H-ZSM-5 zeolite. *Catal. Sci. Technol.* **2019**, *9*, 366–376. [CrossRef]
119. Bedard, J.; Chiang, H.; Bhan, A. Kinetics and mechanism of acetic acid esterification with ethanol on zeolites. *J. Catal.* **2012**, *290*, 210–219. [CrossRef]
120. Schweidtmann, A.M.; Clayton, A.D.; Holmes, N.; Bradford, E.; Bourne, R.A.; LApkin, A.A. Machine learning meets continuous flow chemistry: Automated optimization towards the Pareto front of multiple objectives. *Chem. Eng. J.* **2018**, *352*, 277–282. [CrossRef]
121. Romero Ojeda, G.D.; Esquenazi, E.N.; Gomes, G.J.; Peruchena, N.M.; Zalazar, M.F. Mechanism insight into esterification of levulinic acid with methanol on H-Beta Zeolite: A DFT study. *Catal. Today* **2025**, *445*, 115047. [CrossRef]
122. Wiederkehr, B.; Mitchell, D.A.; de Lima Luz, L.F., Jr.; Krieger, N. Use of the Langmuir–Hinshelwood–Hougen–Watson equation to describe the ethyl esterification of fatty acids catalyzed by a fermented solid with lipase activity. *Biochem. Eng. J.* **2021**, *168*, 107936. [CrossRef]
123. Vu, H.-T.; Lavrič, Ž.; Kostyniuk, A.; Dražić, G.; Grilc, M.; Likozar, B.; Zabukovec Logar, N.; Djinović, P.; Novak Tušar, N. Innovative microkinetic modelling-supported structure–activity analysis of Ni/ZSM-5 during vapor-phase hydrogenation of levulinic acid. *Chem. Eng. J.* **2024**, *495*, 153456. [CrossRef]
124. Ketzer, F.; de Castilhos, F. An assessment on kinetic modeling of esterification reaction from oleic acid and methyl acetate over USY zeolite. *Microporous Mesoporous Mater.* **2021**, *314*, 110890. [CrossRef]
125. Wei, Y.; Lei, H.; Zhu, L.; Zhang, X.; Yadavalli, G.; Liu, Y.; Yan, D. Oxygen-containing fuels from high acid water phase pyrolysis bio-oils by ZSM−5 catalysis: Kinetic and mechanism studies. *Energies* **2015**, *8*, 5898–5915. [CrossRef]
126. Ahmad, K.A.; Elahi, S.F.; Znad, H.; Ahmad, E. Kinetic and mechanistic investigation of butyl levulinate synthesis on ZSM-5 supported phosphomolybdic acid. *Sci. Rep.* **2025**, *15*, 9637. [CrossRef]

127. Kirumakki, S.R.; Nagaraju, N.; Narayanan, S. A comparative esterification of benzyl alcohol with acetic acid over zeolites Hβ, HY and HZSM5. *Appl. Catal. A Gen.* **2004**, *273*, 1–9. [CrossRef]
128. Abbas, A.S.; Albayati, T.M.; Alismaeel, Z.T.; Doyle, A.M. Kinetics and mass transfer study of oleic acid esterification over prepared nanoporous HY zeolite. *Iraqi J. Chem. Pet. Eng.* **2016**, *17*, 47–60. [CrossRef]
129. Schildhauer, T.J.; Hoek, I.; Kapteijn, F.; Moulijn, J.A. Zeolite BEA catalysed esterification of hexanoic acid with 1-octanol: Kinetics, side reactions and the role of water. *Appl. Catal. A* **2009**, *358*, 141–145. [CrossRef]
130. Hoo, P.; Abdullah, A.Z. Kinetics modeling and mechanism study for selective esterification of glycerol with lauric acid using 12-tungstophosphoric acid post-impregnated SBA-15. *Ind. Eng. Chem. Res.* **2015**, *54*, 7852–7858. [CrossRef]
131. Vasconcelos, S.C.; Pinhel, L.F.C.; Madriaga, V.G.C.; Rossa, V.; Batinga, L.G.S.; Silva, D.S.A.; dos Santos, R.D.; Soares, A.V.H.; Urquieta-González, E.A.; Passos, F.B.; et al. Selective synthesis of levulinic ester from furfural catalyzed by hierarchical zeolites. *Catalysts* **2022**, *12*, 783. [CrossRef]
132. Gomes, G.J.; Zalazar, M.F.; Arroyo, P.A. New Insights into the effect of the zeolites framework topology on the esterification reactions: A comparative study from experiments and theoretical calculations. *Top. Catal.* **2022**, *65*, 871–886. [CrossRef]
133. Bakhtiyorov, A.; Elmanov, A.; Maksudov, O.; Norkobilov, A. Comparative analysis of esterification reaction in continuous stirred tank and plug-flow reactors. *Eng. Proc.* **2023**, *56*, 236. [CrossRef]
134. Itoh, N.; Ishida, J.; Sato, T.; Hasegawa, Y. Vapor phase esterification using a CHA type of zeolite membrane. *Catal. Today* **2016**, *268*, 79–84. [CrossRef]
135. Sekine, Y.; Sakai, M.; Matsukata, M. Esterification of acetic acid by flow-type membrane reactor with AEI zeolite membrane. *Membranes* **2023**, *13*, 111. [CrossRef] [PubMed]
136. Bernal, M.P.; Coronas, J.; Menéndez, M.; Santamaría, J. Coupling of reaction and separation at the microscopic level: Esterification processes in a H-ZSM-5 membrane reactor. *Chem. Eng. Sci.* **2002**, *57*, 1557–1562. [CrossRef]
137. De la Iglesia, Ó.; Mallada, R.; Menéndez, M.; Coronas, J. Continuous zeolite membrane reactor for esterification of ethanol and acetic acid. *Chem. Eng. J.* **2007**, *131*, 35–39. [CrossRef]
138. Daramola, M.O.; Aransiola, E.F.; Ojumu, T.V. Potential applications of zeolite membranes in reaction coupling separation processes. *Materials* **2012**, *5*, 2101–2136. [CrossRef]
139. Wu, X.; Li, Y.; Yang, Z.; Peng, M.; Gui, T.; Chen, X.; Kita, H. Intensified esterification of oleic acid and n-butanol using a beta zeolite membrane reactor at low temperature. *Fuel* **2025**, *388*, 134510. [CrossRef]
140. Farsad, A.; Lawson, S.; Rezaei, F.; Rownaghi, A.A. Oxidative dehydrogenation of propane over 3D printed mixed metal oxides/H-ZSM-5 monolithic catalysts using CO_2 as an oxidant. *Catal. Today* **2021**, *374*, 173–174. [CrossRef]
141. Lefevere, J.; Mullens, S.; Meynen, V. The impact of formulation and 3D-printing on the catalytic properties of ZSM-5 zeolite. *Chem. Eng. J.* **2018**, *349*, 260–268. [CrossRef]
142. Li, X.; Rezaei, F.; Rownaghi, A.A. Methanol-to-olefin conversion on 3D-printed ZSM-5 monolith catalysts: Effects of metal doping, mesoporosity and acid strength. *Microporous Mesoporous Mater.* **2019**, *276*, 1–12. [CrossRef]
143. Bogdan, E.; Michorczyk, P. 3D printing in heterogeneous catalysis—The state of the art. *Materials* **2020**, *13*, 4534. [CrossRef]
144. Du, Q.; Bao, S.; Wang, K.; Sheng, Z.; Li, C.; Wu, B.; Liu, K.; Gao, X.; Mao, J.; Zhao, T.-S.; et al. Recent advances in 3D printing of tailored catalysts for heterogeneous thermocatalytic reactions. *Fuel* **2026**, *405*, 136554. [CrossRef]
145. Baroi, C.; Dalai, A.K. Esterification of free fatty acids of green seed canola oil using H-Y zeolite supported 12-tungstophosphoric acid. *Appl. Catal. A Gen.* **2014**, *485*, 99–107. [CrossRef]
146. Dal Pozzo, D.M.; dos Santos, J.A.A.; Júnior, E.S.; Santos, R.F.; Feiden, A.; de Souza, S.N.M.; Burgardt, I. Free fatty acids esterification catalyzed by acid faujasite-type zeolite. *RSC Adv.* **2019**, *9*, 4900–4907. [CrossRef]
147. Abdullah, S.H.Y.S.; Hanapi, N.H.M.; Azid, A.; Umar, R.; Juahir, H.; Khatoon, H.; Endut, A. A review of biomass-derived heterogeneous catalyst for a sustainable biodiesel production. *Renew. Sustain. Energy Rev.* **2017**, *70*, 1040–1051. [CrossRef]
148. Thangaraj, B.; Solomon, P.R.; Muniyandi, B.; Ranganathan, S.; Lin, L. Catalysis in biodiesel production—A review. *Clean Energy* **2019**, *3*, 2–23. [CrossRef]
149. Yoldi, M.; Fuentes-Ordoñez, E.G.; Korili, S.A.; Gil, A. Zeolite synthesis from industrial wastes. *Microporous Mesoporous Mater.* **2019**, *287*, 183–191. [CrossRef]
150. Lin, Y.-J.; Chen, J.-C. Resourcization and valorization of waste incineration fly ash for the synthesis of zeolite and applications. *J. Environ. Chem. Eng.* **2021**, *9*, 106549. [CrossRef]
151. Cao, C.; Xuan, W.; Yan, S.; Wang, Q. Zeolites synthesized from industrial and agricultural solid waste and their applications: A review. *J. Environ. Chem. Eng.* **2023**, *11*, 110898. [CrossRef]
152. Bello, M.O.; Abdus-Salam, N.; Adekola, F.A.; Oyewumi-Musa, R.T.; Pal, U. Synthesis and characterization of zeolite Y from agricultural and municipal wastes: A waste management approach. *Waste Manag. Bull.* **2024**, *2*, 122–129. [CrossRef]
153. Zhang, W.; Zhang, T.; Lv, Y.; Jing, T.; Gao, X.; Gu, Z.; Li, S.; Ao, H.; Fang, D. Recent progress on the synthesis and applications of zeolites from industrial solid wastes. *Catalysts* **2024**, *14*, 734. [CrossRef]

154. Zhao, Y.; Gu, S.; Li, L.; Wang, M. From waste to catalyst: Growth mechanisms of ZSM-5 zeolite from coal fly ash & rice husk ash and its performance as catalyst for tetracycline degradation in Fenton-like oxidation. *Environ. Pollut.* **2024**, *345*, 123509. [CrossRef]
155. Shin, S.; Kim, M.J. Hydrothermal synthesis of zeolites from residual waste generated via indirect carbonation of coal fly ash. *Sustain. Environ. Res.* **2024**, *34*, 1. [CrossRef]
156. Bozell, J.J.; Moens, L.; Elliott, D.C.; Wang, Y.; Neuenschwander, G.G.; Fitzpatrick, S.W.; Bilski, R.J.; Jarnefeld, J.L. Production of levulinic acid and use as a platform chemical for derived products. *Resour. Conserv. Recycl.* **2000**, *28*, 227–239. [CrossRef]
157. Kohli, K.; Prajapati, R.; Sharma, B.K. Bio-based chemicals from renewable biomass for integrated biorefineries. *Energies* **2019**, *12*, 233. [CrossRef]
158. Zheng, B.; Yu, S.; Chen, Z.; Huo, Y.-X. A consolidated review of commercial-scale high-value products from lignocellulosic biomass. *Front. Microbiol.* **2022**, *13*, 933882. [CrossRef]
159. Costa, B.E.B.; da Silva, A.O.S.; Meneghetti, S.M.P. Esterification of levulinic acid with different alcohols using mesoporous stannosilicates as the catalyst. *ACS Omega* **2024**, *9*, 31128–31135. [CrossRef]
160. Chung, K.-H.; Chang, D.-R.; Park, B.-G. Removal of free fatty acid in waste frying oil by esterification with methanol on zeolite catalysts. *Bioresour. Technol.* **2008**, *99*, 7438–7443. [CrossRef]
161. Avhad, M.R.; Marchetti, J.M. A review on recent advancement in catalytic materials for biodiesel production. *Renew. Sustain. Energy Rev.* **2015**, *50*, 696–718. [CrossRef]
162. Luque, R.; Clark, J.H. Biodiesel-like biofuels from simultaneous transesterification/esterification of waste oils with a biomass-derived solid acid catalyst. *Chem. Cat. Chem.* **2010**, *2*, 1077–1081. [CrossRef]
163. Verma, P.; Kuwahara, Y.; Mori, K.; Raja, R.; Yamashita, H. Functionalized mesoporous SBA-15 silica: Recent trends and catalytic applications. *Nanoscale* **2020**, *12*, 11333–11363. [CrossRef] [PubMed]
164. Endalew, A.K.; Kiros, Y.; Zanzi, R. Inorganic heterogeneous catalysts for biodiesel production from vegetable oils. *Biomass Bioenergy* **2011**, *35*, 3787–3809. [CrossRef]
165. Miądlicki, P.; Wróblewska, A.; Kiełbasa, K.; Koren, Z.C.; Michalkiewicz, B. Sulfuric acid modified clinoptilolite as a solid green catalyst for solvent-free α-pinene isomerization process. *Microporous Mesoporous Mater.* **2021**, *324*, 111266. [CrossRef]
166. Fajdek-Bieda, A.; Wróblewska, A.; Miądlicki, P.; Tołpa, J.; Michalkiewicz, B. Clinoptilolite as a natural, active zeolite catalyst for the chemical transformations of geraniol. *Reac. Kinet. Mech. Cat.* **2021**, *133*, 997–1011. [CrossRef]
167. Grzeszczak, J.; Wróblewska, A.; Kiełbasa, K.; Koren, Z.C.; Michalkiewicz, B. The application of clinoptilolite as the green catalyst in the solvent-free oxidation of α-Pinene with oxygen. *Sustainability* **2023**, *15*, 10381. [CrossRef]
168. Sobuś, N.; Czekaj, I. Comparison of synthetic and natural zeolite catalysts' behavior in the production of lactic acid and ethyl lactate from biomass-derived dihydroxyacetone. *Catalysts* **2021**, *11*, 1006. [CrossRef]
169. Rodríguez-Iznaga, I.; Shelyapina, M.G.; Petranovskii, V. Ion exchange in natural clinoptilolite: Aspects related to its structure and applications. *Minerals* **2022**, *12*, 1628. [CrossRef]
170. Basyouny, M.G.; Abukhadra, M.R.; Alkhaledi, K.; El-Sherbeeny, A.M.; El-Meligy, M.A.; Soliman, A.T.A.; Luqman, M. Insight into the catalytic transformation of the waste products of some edible oils (corn oil and palm oil) into biodiesel using MgO/clinoptilolite green nanocomposite. *Mol. Catal.* **2021**, *500*, 111340. [CrossRef]
171. Aghel, B.; Gouran, A.; Nasirmanesh, F. Transesterification of waste cooking oil using clinoptilolite/industrial phosphoric waste as green and environmental catalysts. *Energy* **2022**, *244*, 123138. [CrossRef]
172. Lycourghiotis, S.; Kordouli, E. Biomass conversion to value-added chemicals and fuels using natural minerals as catalysts or catalytic supports. *Catalysts* **2025**, *15*, 1006. [CrossRef]